REVIEW

Mechanistic Studies of Metal Aqua Ions: A Semi-Historical Perspective

by **Stephen F. Lincoln**

Department of Chemistry, University of Adelaide, Adelaide, SA 5005 Australia
(phone: +61 8 8303 5559; fax: +61 8 8303 4358; e-mail: stephen.lincoln@adelaide.edu.au)

Dedicated to Professor *André Merbach*, a fine man and scientist, and a friend and colleague for twenty-five years, on the occasion of his 65th birthday

A semi-historical review of the establishment of the nature of metal aqua ions ranging from the alkali metal ions to the lanthanides and the mechanism of water exchange and ligand substitution on them is presented.

1. Introduction. – The oceans cover 71% of Earth's surface and contain vast quantities of the simplest metal complex, the metal aqua ion. However, while the pioneering work of *Werner* and *Jørgensen* on the colorful cobalt(III) complexes in the late nineteenth and early twentieth centuries [1–3] established an early understanding of coordination chemistry which was to burgeon into the vast panoply that it is today [4][5], the nature of the metal aqua ion remained an enigma. This was largely because the ability to distinguish coordinated water from bulk water had to await the arrival of methodologies which arose from the technological acceleration of the Second World War. Particularly important among these were the isotopic enrichment of water, and NMR and ultrasonic spectroscopy. A major breakthrough came in 1951 when *Hunt* and *Taube* determined the coordination number and the water-exchange rate of inert $[Cr(H_2O)_6]^{3+}$ using $^{18}OH_2$ mass spectrometry [6]. Contemporaneously, *Eigen* developed ultrasonic and other fast-reaction techniques to characterize ligand-substitution processes on very labile metal aqua ions, which led to estimates of water lability in their first coordination spheres [7]. In 1958, *Hunt* and *Taube* determined the first volume of activation, $\Delta V^{\ddagger}$ ($= +1.2$ cm^3 mol^{-1}), for water exchange on $[Co(NH_3)_5H_2O]^{3+}$, a parameter which was to prove of great mechanistic value [8]. Another major advance came in 1962 with the adaptation of the *Bloch* equations by *Swift* and *Connick* to accommodate quantitative water-exchange studies of paramagnetic metal aqua ions by using ^{17}O-NMR spectroscopy [9]. As the sophistication of experimentation increased, so did the level of mechanistic discussion, and it became increasingly apparent that $\Delta V^{\ddagger}$ studies could greatly enhance the mechanistic interpretation gained from other water-exchange and ligand-substitution kinetic parameters. This led to the pioneering studies of water- and other solvent-exchange processes on both inert and labile metal ions by means of variable-pressure NMR methods by *Merbach* [10][11]. Such has been the impact of this work that it has become the benchmark whereby water- and other solvent-exchange and ligand-substitution studies are assessed.

In parallel with the evolution of kinetic methodologies and mechanistic understanding, the development of physical methods for determining the structures of metal aqua ions and computational methods for simulating water-exchange processes added greatly to the attainment of the powerful understanding of the metal aqua ions that now exists [12–16].

2. The Variation of Lability of Metal Aqua Ions. – Water exchange between the first and second coordination spheres of a metal aqua ion may be represented by *Eqn. 1* where the asterisk is a typographical distinction only; k_{H_2O} is the observed first-order exchange-rate constant for a particular H_2O molecule in the first coordination sphere, and the water-exchange rate on $[M(H_2O)_n]^{m+}$ is given by *Eqn. 2*. ($\tau_{H_2O} = 1/k_{H_2O}$ is the mean residence time of a particular H_2O molecule in the first coordination sphere).

$$[M(H_2O)_n]^{m+} + H_2O^* \overset{k_{H_2O}}{\rightleftharpoons} [M(H_2O)_{(n-1)}H_2O^*]^{m+} + H_2O \quad (1)$$

$$\text{Water exchange rate} = nk_{H_2O}[M(H_2O)_n^{m+}] \quad (2)$$

The values of k_{H_2O} (298.2 K) and τ_{H_2O} vary over almost 20 orders of magnitude, as shown in *Fig. 1*, which is an updated version of the Figure first published by *Eigen* in 1963 [7]. At the slow extreme of lability is $[Ir(H_2O)_6]^{3+}$ for which τ_{H_2O} (298 K) $= 9.1 \cdot 10^9$ s which corresponds to *ca.* 300 years and water exchange occurring every *ca.* 50 years [17]. At the fast extreme is $[Eu(H_2O)_7]^{2+}$ with τ_{H_2O} (298 K) $= 2.0 \cdot 10^{-10}$ s during which light travels *ca.* 6 cm and a water-exchange event occurs every *ca.* $2.9 \cdot 10^{-11}$ s [18]. Generally, the greatest lability is shown by metal aqua ions of large ionic radius, r_M [19], and low charge that together result in a low surface-charge density. An additional factor, the electronic occupancy of the *d*-orbitals, has a major effect on the lability of the transition-metal ions [20–22]. Generally, three major categories of metal aqua ions are distinguishable: *i*) the main-group-metal ions, *ii*) the transition-metal ions, and *iii*) the trivalent lanthanide ions.

The labilities of the main-group-metal aqua ions increase with decrease in surface-charge density and increase in coordination number [7][12][15][16]. Thus, the high labilities of the alkali-metal ions are encompassed by about one order of magnitude variation as lability increases from $[Li(OH_2)_6]^+$ to $[Rb(OH_2)_6]^+$ to $[Cs(H_2O)_8]^+$. The alkaline-earth-metal aqua ions show six orders of magnitude variation in lability with $[Be(H_2O)_4]^{2+}$ being the least labile and lability increasing through $[Mg(H_2O)_6]^{2+}$, $[Ca(H_2O)_8]^{2+}$, $[Sr(H_2O)_8]^{2+}$ to $[Ba(H_2O)_8]^{2+}$. The high surface-charge density of Al^{3+} causes the lability of $[Al(H_2O)_6]^{3+}$ to fall in the middle of the range of *Fig. 1*, while lability increases 10^6 fold to $[In(H_2O)_6]^{3+}$ as surface-charge density decreases as the group is descended.

The transition-metal aqua ions are six-coordinate, with the exception of $[Cu(H_2O)_5]^{2+}$ and square-planar $[Pd(H_2O)_4]^{2+}$ and $[Pt(H_2O)_4]^{2+}$, and encompass almost 20 orders of magnitude in lability because of the effects of their d-orbital electronic occupancies superimposing on the influence of surface-charge density [20–22]. (The d^{10} $[Zn(H_2O)_6]^{2+}$, $[Cd(H_2O)_6]^{2+}$, and $[Hg(H_2O)_6]^{2+}$ ions behave similarly to main-group-metal aqua ions and their labilities increase by two orders of magnitude as the group is descended.) In contrast, the different electronic f-orbital occupancies of

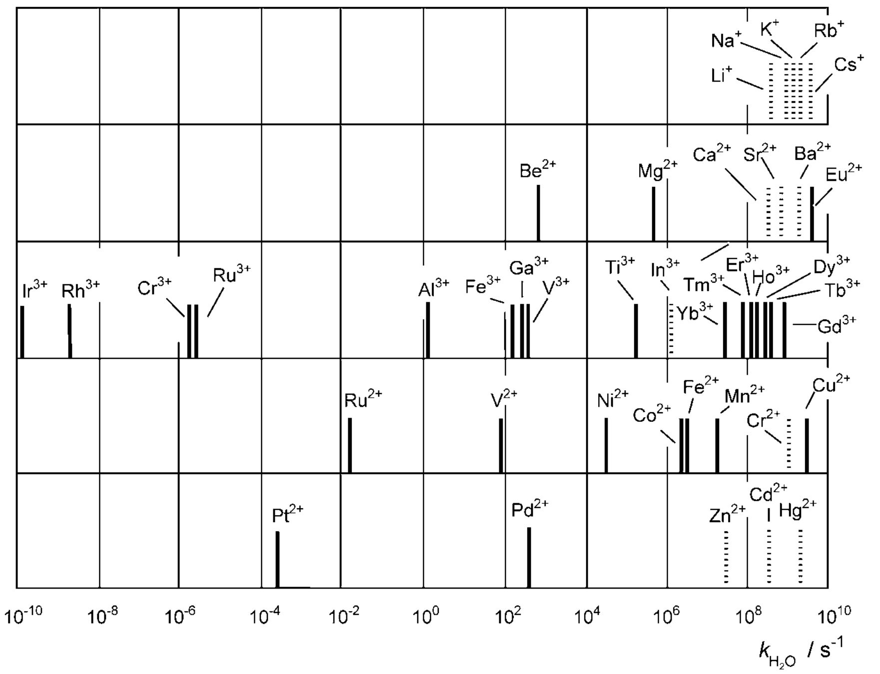

Fig. 1. *Water-exchange rate constants,* k_{H_2O}*, for a particular water molecule in the first coordination sphere of* $[M(H_2O)_n]^{m+}$. Bold bars represent directly determined k_{H_2O} values while hashed bars indicate k_{H_2O} values estimated from ligand-substitution studies.

the trivalent lanthanide ions (Ln^{3+}) have only a very small effect on their lability, which is encompassed within two orders of magnitude and is dominated by their large r_M which decrease along with lability, as atomic number increases [23–25].

The only directly determined τ_{H_2O} of a H_2O molecule exchanging between the second coordination sphere and bulk water is $1.28 \cdot 10^{-10}$ s (k_{H_2O} (298 K) $= 7.8 \cdot 10^9$ s^{-1}, $\Delta H^{\ddagger} = 21.3$ kJ mol^{-1}, $\Delta S^{\ddagger} = +16.2$ J K^{-1} mol^{-1}) for $[Cr(H_2O)_6]^{3+}$ which compares with $k_{H_2O} = 6.9 \cdot 10^9$ s^{-1} obtained from molecular-dynamics calculations [26]. It was similarly shown that $\tau_{H_2O} = 1.3 \cdot 10^{-11}$, $1.2 \cdot 10^{-11}$, and $1.8 \cdot 10^{-11}$ s for H_2O in the second coordination sphere of Nd^{3+}, Sm^{3+}, and Yb^{3+}, respectively [15][23]. These data are consistent with water exchange between the second coordination sphere and bulk water being close to diffusion control.

3. The Evolution of Mechanistic Interpretation of Water Exchange and Ligand Substitution on Metal Aqua Ions. – Due to the paucity of knowledge about metal aqua ions, early mechanistic discussion was largely confined to ligand-substitution processes which induced a color change or other change. Such discussion largely followed the organic mechanistic concepts of unimolecular and bimolecular nucleophilic substitution, S_{N1} and S_{N2}, at C-centers and was mainly confined to inert metal complexes as discussed in the seminal books by *Basolo* and *Pearson* in 1957 and 1967 [27]. With the advent of fast-reaction techniques, the scope for mechanistic interpretation broadened, and it became apparent that, for a particular ligand X^{x-}, which substitutes into the first coordination sphere of $[M(H_2O)_n]^{m+}$, the substitution rate shows a similar variation with the nature of M^{m+} as does water exchange. This infers that the mechanisms of both processes are similar. It is only for the most-labile metal aqua ions that the rates of water exchange and ligand substitution in the first coordination sphere are within an order of magnitude of the rates of water exchange and ligand substitution into the second coordination sphere from bulk water. Thus, rate-determining water-exchange and ligand-substitution events usually occur in the first coordination sphere of $[M(H_2O)_n]^{m+}$, and substitution by a ligand X^{x-} is preceded by its entry into the second coordination sphere to form an encounter or outer-sphere complex $[M(H_2O)_n]\cdot X^{(m-x)}$ at close to diffusion-controlled rates.

It is seldom the case that more than one stage of the transfer of a monodentate ligand X^{x-} from bulk water to the first coordination sphere is detected other than by the ultrasonic method where up to three steps have been detected as in the *Eigen–Tamm* mechanism shown in *Eqn. 3* [28]. Here, **0** represents M^{m+} and X^{x-} separated by more than two H_2O molecules, **1** represents M^{m+} and X^{x-} separated by two H_2O molecules, **2** represents M^{m+} and X^{x-} separated by one H_2O molecule in the encounter complex, and **3** represents M^{m+} and X^{x-} in contact in the new complex $[M(H_2O)_{(n-1)}X]^{(m-x)+}$. The diffusion-controlled formation of **1** (k_{01}/k_{10}) is followed by the fast formation of **2** (k_{12}/k_{21}), which leads to the slower formation of **3** (k_{23}/k_{32}). Usually, the formation of **1** is not detected, and the simplified sequence of the *Eigen–Wilkins* mechanism (*Eqn. 4*) is discussed instead [29][30].

$$\underset{\mathbf{0}}{M^{m+} + X^{x-}} \underset{k_{10}}{\overset{k_{01}}{\rightleftharpoons}} \underset{\mathbf{1}}{M\cdot OH_2\cdot OH_2\cdot X^{(m-x)+}} \underset{k_{21}}{\overset{k_{12}}{\rightleftharpoons}} \underset{\mathbf{2}}{M\cdot OH_2\cdot X^{(m-x)+}} \underset{k_{32}}{\overset{k_{23}}{\rightleftharpoons}} \underset{\mathbf{3}}{MX^{(m-x)+}} \tag{3}$$

$$M^{m+} + X^{x-} \underset{k_{21}}{\overset{k_{12}}{\rightleftharpoons}} M\cdot OH_2\cdot X^{(m-x)+} \underset{k_{32}}{\overset{k_{23}}{\rightleftharpoons}} MX^{(m-x)+} \tag{4}$$

$$k_{obs} = \{(k_{23}K_{12}[X^{x-}])/(1 + K_{12}[X^{x-}]) + k_{32} \tag{5}$$

The sequential equilibria in *Eqn. 4* are characterized by $K_{12} = k_{12}/k_{21}$ (often denoted as K_o) and $K_{23} = k_{23}/k_{32}$, respectively. When K_{12} cannot be directly determined, it is frequently estimated through the *Fuoss* equation [31]. Often, it is only possible to characterize the kinetics of the second equilibrium of *Eqn. 4*. Irrespective of the intimate mechanism of ligand substitution, the pseudo-first-order rate constant for the approach to equilibrium, k_{obs}, is given by *Eqn. 5* when $[X^{x-}] \gg [M^{m+}]$. When K_{12} $[X^{x-}] \ll 1$, $k_{obs} \approx k_{23}\ K_{12}\ [X^{x-}] + k_{32}$, and when $K_{12}\ [X^{x-}] \gg 1$, $k_{obs} \approx k_{23} + k_{32}$, where k_{23} and k_{32} characterize the interchange of X^{x-} between the first and second coordination spheres. Equivalent expressions apply when $[M^{m+}] \gg [X^{x-}]$. When K_{12} does not differ significantly from that arising from diffusive collisions, the equilibrium described by K_{12}

may be ignored, and the substitution of X^{x-} on M^{m+} to form $MX^{(m-x)+}$ is described by k_{23} alone. (This situation appears to apply for the ligand substitutions on $[Pd(H_2O)_4]^{2+}$ and $[Pt(H_2O)_4]^{2+}$ discussed in *Sect. 11.*) It is within this kinetic framework that the intimate mechanisms of the water-exchange and ligand-substitution processes have to be identified. For the sake of uniformity, the symbolism of *Eqn. 5* is used in subsequent discussion of ligand substitution, where k_{23} is used to indicate the ligand-substitution step, although other symbolism may have been used in the original report.

4. The Classification of Water-Exchange and Ligand-Substitution Mechanisms. – Since 1965, a new formalism proposed by *Langford* and *Gray*, in which the associative and dissociative mechanisms, **A** and **D**, respectively, represent the mechanistic extremes for the substitution of a H_2O molecule in $[M(H_2O)_n]^{m+}$ by X^{x-}, rapidly became the vehicle for mechanistic discussion [32]. In the **A** mechanism, $[M(H_2O)_n]^{m+}$ and X^{x-} pass through a first transition state to form a reactive intermediate $[M(H_2O)_nX]^{(m-x)+}$, where the coordination number of M^{m+} is increased by one. This intermediate survives several molecular collisions before passing through a second transition state to form the product $[M(H_2O)_{(n\text{-}1)}X]^{(m-x)+}$. The rate-determining step is the bond making between M^{m+} and X^{x-}, and the mechanism is associatively (**a**) activated. The **D** mechanism operates when $[M(H_2O)_n]^{m+}$ passes through a first transition state to form a reactive intermediate $[M(H_2O)_{(n-1)}]^{m+}$, where the coordination number of M^{m+} is decreased by one. This intermediate also survives several molecular collisions before passing through a second transition state to form the product $[M(H_2O)_{(n-1)}X]^{(m-x)+}$. The rate determining step is bond breaking, and the mechanism is dissociatively (**d**) activated. Both of these mechanisms may occur within an encounter complex (*Eqn. 5*).

Between the **A** and **D** extremes, a continuum of mechanisms exists in which the entering and leaving ligands make varying contributions to the transition-state energetics. They range from the **a**-activated associative interchange mechanism $\mathbf{I_a}$, where bond making is dominant, through the interchange mechanism **I**, where bond making and breaking are similarly important, to the **d**-activated interchange mechanism $\mathbf{I_d}$, where bond breaking is dominant. In principle, distinction between the **a**- and **d**-activation modes of the **A** to **D** mechanistic continuum is possible through a comparison of k_{H_2O} for $[M(OH_2)_n]^{m+}$ and k_{23} for X^{x-} substitution. The X^{x-} substitution k_{23} may vary from being much less than to much greater than k_{H_2O} for the **A** mechanism with corresponding variations in $\Delta H^{\ddagger}$ and $\Delta S^{\ddagger}$ which reflect the variation of the new bond made in the transition state. In contrast, k_{23} cannot be greater than k_{H_2O} and may be significantly less for the **D** mechanism as a consequence of statistical factors [33–36]. Also, $\Delta H^{\ddagger}$ should be close to that for the water-exchange process. Within these extremes, the selectivity for X^{x-} should decrease from the **A** mechanism through the $\mathbf{I_a}$, **I**, and $\mathbf{I_d}$ mechanisms to the **D** mechanism. These guidelines are constrained by either the X^{x-} selectivity range being significantly contracted for X^{x-} hard bases substituting on M^{m+} hard acids [37], or the rate of water exchange on $[M(OH_2)_n]^{m+}$ approaching diffusion control ($k_{H_2O} \approx 3.6 \cdot 10^{11}\ s^{-1}$) and high X^{x-} substitution rates occurring with little selectivity. For each mechanism, microscopic reversibility requires that the same reaction coordinate should be traversed from left to right and *vice versa* so that the same mechanism operates in both directions.

In similar systems, **a**-activated substitutions tend to have smaller $\Delta H^{\ddagger}$ magnitudes than do **d**-activated substitutions, and $\Delta S^{\ddagger}$ tends to be negative and positive for **a**- and **d**-activated substitutions, respectively [38]. Even so, it is often difficult to find a series of similar ligand substitutions from which mechanistic deductions may be made from $\Delta H^{\ddagger}$ and $\Delta S^{\ddagger}$. Fortunately, the volume of activation $\Delta V^{\ddagger}$ has proven to be a particularly powerful parameter through which water- and other solvent-exchange and some ligand-substitution mechanisms may be assigned [12][15][16][39–42].

5. The Volume of Activation. – The $\Delta V^{\ddagger}$ for water exchange on $[M(H_2O)_n]^{m+}$ is particularly amenable to mechanistic interpretation as the redistribution of charge on going from the ground-state to the transition state is minimal. Thus, the pressure dependence of k_{H_2O} is given by *Eqn. 6* where $\Delta V^{\ddagger}$ is the difference between the partial molar volumes of the ground and transition states. An approximate solution to *Eqn. 6* is given by *Eqn. 7* in which $k_{(P)H_2O}$ and $k_{(0)H_2O}$ are the rate constants at an applied and ambient pressure, respectively. The $\Delta\beta^{\ddagger}P^2/2RT$ term, where $\Delta\beta^{\ddagger}$ is the compressibility of the transition state, is usually insignificant for water exchange over applied pressures of up to 200 Mpa so that $\Delta V^{\ddagger} \approx \Delta V_{(0)}$. Two components, $\Delta V^{\ddagger}_{\text{intrinsic}}$, arising from changes in bond distances and angles as the transition state is approached, and $\Delta V^{\ddagger}_{\text{electrostriction}}$, arising from accompanying water electrostriction effects, make up $\Delta V^{\ddagger}$. Water is highly electrostricted, and no significant charge distribution occurs in the water-exchange transition state such that $\Delta V^{\ddagger}_{\text{electrostriction}} \approx 0$ and $\Delta V^{\ddagger}_{\text{intrinsic}} \approx \Delta V^{\ddagger}$, which is a direct reflection of the extent of bond making and breaking occurring in the transition-state. (This contrasts with the situation for a ligand-substitution process involving substantial charge redistribution in the transition state such that $\Delta V^{\ddagger}_{\text{electrostriction}}$ dominates $\Delta V^{\ddagger}$ so that the determination of $\Delta V^{\ddagger}_{\text{intrinsic}}$ is less straightforward.)

$$(\delta \ln k_{H_2O}/\delta P)_T = -\Delta V^{\ddagger}/RT \quad (6)$$

$$\ln k_{(P)H_2O} = \ln k_{(0)H_2O} - \Delta V^{\ddagger}_{(0)}P/RT + \Delta\beta^{\ddagger}P^2/2RT \quad (7)$$

When the application of pressure causes k_{H_2O} to increase, $\Delta V^{\ddagger}$ is negative and *vice versa*, and the transition state contracts and expands with respect to the ground state, respectively. Broadly, a contracted transition state involves more bond making than breaking and corresponds to **a**-activation, whereas an expanded transition state involves more bond breaking than making and a **d**-activation mode. The effects of pressure on water exchange according to the mechanism through which it occurs are illustrated by *Fig. 2* [40]. According to this scheme, an **A** mechanism is characterized by a contraction of the transition state as the incoming H_2O molecule enters the first coordination sphere, and $\Delta V^{\ddagger}$ is large and negative. The **D** mechanism is characterized by a substantial expansion of the transition state due to the emergence of the leaving H_2O molecule from the first coordination sphere, and $\Delta V^{\ddagger}$ is large and positive. For the **I** mechanism, equal amounts of bond breaking and bond making balance one another in their contributions so that $\Delta V^{\ddagger} \approx 0$. On either side of the **I** mechanism are the $\mathbf{I_a}$ and $\mathbf{I_d}$ mechanisms where the bond-making contribution to the transition state is greater than the bond-breaking contribution and *vice versa* so that they are characterized by negative and positive $\Delta V^{\ddagger}$ values, respectively. Thus, both the sign and magnitude of

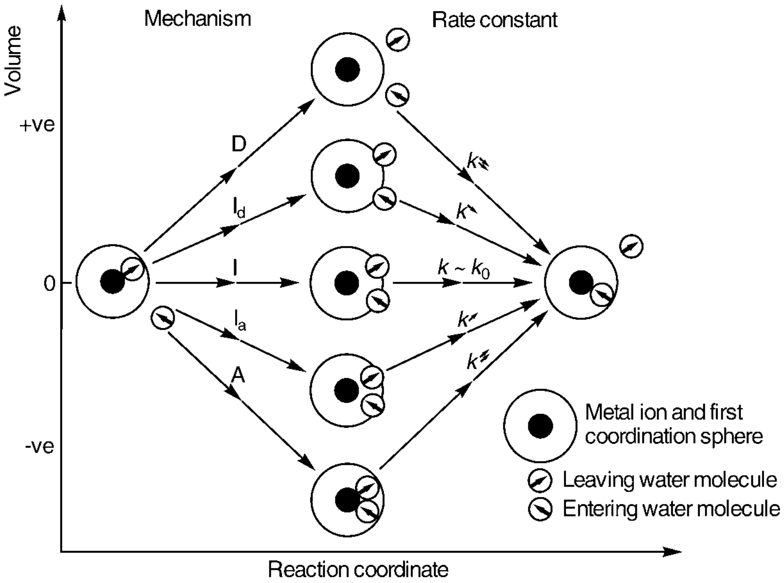

Fig. 2. *Representation of the ground states and transition states for water exchange on* $[M(H_2O)_n]^{m+}$. The upward inclination of the arrow superscript of k_{H_2O} indicates that increased applied pressure accelerates the exchange process and *vice versa* for a downward inclination. Two superscript arrows indicate that the effect of pressure on k_{H_2O} is large and the magnitude of $\Delta V^{\ddagger}$ is large. A single superscript arrow indicates a lesser effect of pressure on k_{H_2O} and a lesser magnitude of $\Delta V^{\ddagger}$. Adapted from [40].

$\Delta V^{\ddagger}$ changes as the contributions of bond making and bond breaking in the transition-state change.

6. Quantitative Approaches to the Interpretation of Activation Volumes. – No experimental method is available to detect the reactive intermediate species characterizing **A** and **D** mechanisms for water exchange on $[M(H_2O)_n]^{m+}$ and to distinguish them from $\mathbf{I_a}$ and $\mathbf{I_d}$ mechanisms, respectively. In 1983, *Swaddle* suggested that a *Moore–O'Ferrall* diagram may be used to illustrate the volume changes along the reaction coordinate as the transition state is approached as shown in *Fig. 3,a* [39][41]. For water exchange, the sides of the diagram represent the change in bond order for the M^{m+} to entering and leaving H_2O from 0 to 1 in the exchange reaction in *Eqn. 1*. The transition states lie on the diagonal joining the corners at which the transition states/reactive intermediates for the extreme **A** and **D** water-exchange mechanisms, $[M(H_2O)_{(n+1)}]^{m+}$ and $[M(H_2O)_{(n-1)}]^{m+}$, respectively, are located. The magnitude and sign of $\Delta V^{\ddagger}$ is the sum of the volume changes arising from the bond-making and -breaking contributions. *Swaddle* scaled the diagram using semi-empirical calculations that gave $\Delta V^{\ddagger} = -13.5 \pm 1$ and $+13.5$ cm^3 mol^{-1} for **A** and **D** water-exchange mechanisms, respectively, for the first-row-transition-metal ions $[M(H_2O)_6]^{2+/3+}$ with smaller values for the $\mathbf{I_a}$ and $\mathbf{I_d}$ mechanisms. These values include either an increase or a decrease of r_M by *ca.* 6 pm when n changes from 6 to either 7 or 5, respectively, and show little dependence on r_M.

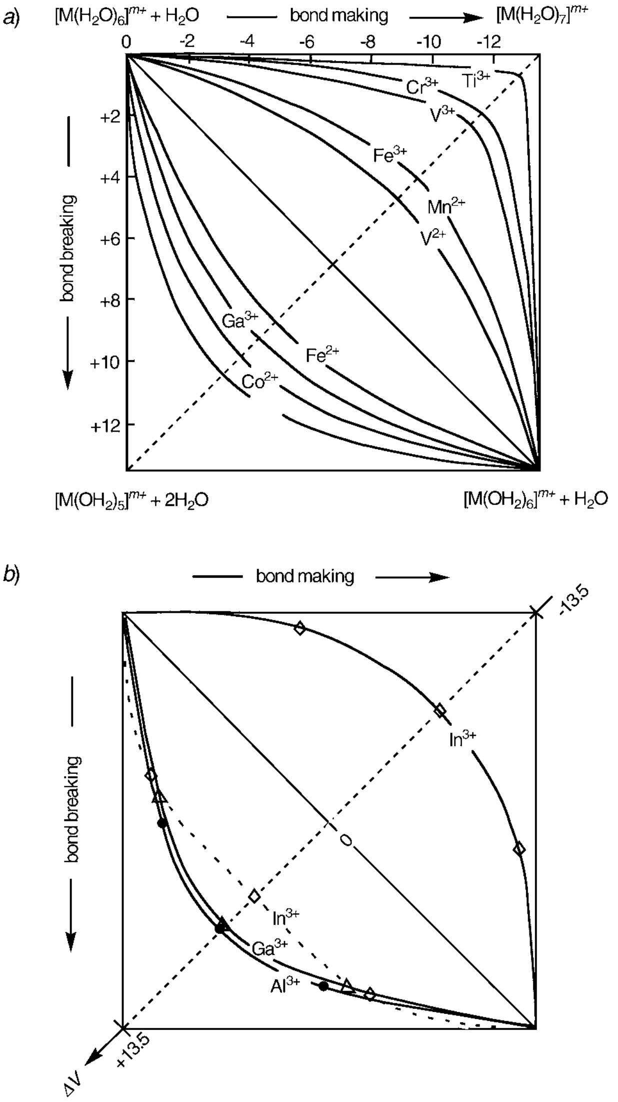

Fig. 3. a) *A* Moore – O'Farrell *depiction of* $\Delta V^{\ddagger}$ *variations along the reaction coordinate for water exchange on* $[M(H_2O)_6]^{2/3+}$ *in terms of bond-making and -breaking contributions in* cm^3 mol^{-1} (adapted from [38]). b) *Volume variations in* cm^3 mol^{-1} *along the reaction coordinate from* ab initio *calculations for* $[Al(H_2O)_6]^{3+}$ *and its* Ga^{3+} *and* In^{3+} *analogues.* The solid and open points on the solid curves lying to either side of the hatched diagonal represent the transition states and those on the diagonal represent the reactive intermediates $[Al(H_2O)_5]^{3+}$, $[Ga(H_2O)_5]^{3+}$, and $[In(H_2O)_7]^{3+}$. The hatched curve for $[In(H_2O)_6]^{3+}$ corresponds to a **D** mechanism for exchange but is disfavored because of the greater activation energy required by comparison with that for the **A** mechanism. Adapted from [42].

In 1998, *Merbach* and co-workers used *ab initio* calculations of volume changes along the reaction coordinate to show that water exchange on $[Al(H_2O)_6]^{3+}$ and $[Ga(H_2O)_6]^{3+}$ involved identical transition states approximately midway between the

D five-coordinate intermediate and the six-coordinate ground state [42]. These transition states lie to either side of the diagonal equivalent to that in *Fig. 3,a* such that $\Delta V^{\ddagger} = +5.6$ and $+4.8$ cm^3 mol^{-1} for $[Al(H_2O)_6]^{3+}$ and $[Ga(H_2O)_6]^{3+}$, respectively, which are close to the experimental values [43][44], and the five-coordinate intermediates lie on the diagonal with $\Delta V = +7.1$ and $+6.9$ cm^3 mol^{-1} as shown in *Fig. 3,b*. Similar calculations for $[In(H_2O)_6]^{3+}$ gave $\Delta V^{\ddagger} = -5.2$ cm^3 mol^{-1} for water exchange through an **A** mechanism involving a seven-coordinate intermediate ($\Delta V = -7.1$ cm^3 mol^{-1}), but there is no experimental $\Delta V^{\ddagger}$ with which comparison may be made. (Trimethyl phosphate (TMP) exchange on $[Al(TMP)_6]^{3+}$ and its Ga^{3+} and In^{3+} analogues is characterized by $\Delta V^{\ddagger} = +22.5$, $+20.7$, and -21.4 cm^3 mol^{-1} consistent with the operation of **D** mechanisms in the first two cases and either an **A** or $\mathbf{I_a}$ mechanism in the third as a consequence of the greater r_M ($= 80$ pm) of In^{3+} [10].)

The extent to which the $M^{m+}-OH_2$ bond distances of the five H_2O molecules in $[M(H_2O)_6]^{m+}$ not directly involved in the exchange process change in the transition state, and the consequent volume change contributed to $\Delta V^{\ddagger}$ has recently been calculated by quantum-mechanical methods [45][46]. For $[Ru(H_2O)_6]^{2+}$, which undergoes water exchange through either a **D** or $\mathbf{I_d}$ mechanism according to these calculations, and $[Rh(H_2O)_6]^{3+}$ and $[Ir(H_2O)_6]^{3+}$, which undergo water exchange with retention of configuration through $\mathbf{I_a}$ mechanisms, these volume-change contributions are -1.7, -0.8, and -0.9 cm^3 mol^{-1}, respectively. Intuitively, the negative volume change is anticipated for a **d**-activated mechanism, while the negative changes for the **a**-activated mechanisms are less expected. When these values are compared with the experimental $\Delta V^{\ddagger}$ of -0.4, -4.2, and -5.7 cm^3 mol^{-1} [17][47][48], it appears that the volume increase arising from bond-breaking by the leaving H_2O molecule is *ca.* $+1.3$ cm^3 mol^{-1} for $[Ru(H_2O)_6]^{2+}$, and the volume decrease occurring for bond making by the entering water molecule in $[Rh(H_2O)_6]^{3+}$ and $[Ir(H_2O)_6]^{3+}$ is *ca.* -3.4 and -4.8 cm^3 mol^{-1}, respectively. Although, on the basis of the experimental $\Delta V^{\ddagger}$ of -0.4 cm^3 mol^{-1}, water exchange on $[Ru(H_2O)_6]^{2+}$ was assigned an **I** mechanism, it appears from these calculations that the contraction of volume due to shortening of five $Ru^{2+}-OH_2$ bonds offsets the increase in volume due to bond breaking by the sixth and leaving H_2O molecule in the transition state.

7. Water Exchange on the Main-Group-Metal Aqua Ions. – The labilities of the main-group-metal aqua ions are dominated by variations in r_M and charge which determine the surface-charge density and coordination number. Thus, apart from the indirectly determined k_{H_2O} shown in *Fig. 1* for the alkali-metal aqua ions, the only other data pertinent to water exchange comes from incoherent quasi-elastic neutron scattering studies which show that water proton residence times on Li^+ and Cs^+ in concentrated aqueous solution are $\leq 10^{-10}$ s. As these residence times reflect both water exchange and proton exchange on coordinated water, these data suggest that $k_{H_2O} \leq 10^{10}$ s^{-1} [49]. The smallest alkaline-earth-metal ion, Be^{2+} ($r_M = 27$ pm), forms tetrahedral $[Be(H_2O)_4]^{2+}$ characterized by directly determined k_{H_2O} (298 K) $= 730$ s^{-1}, $\Delta H^{\ddagger} = 59.2$ kJ mol^{-1}, and $\Delta S^{\ddagger} = +8.4$ J K^{-1} mol^{-1} [50]. The $\Delta V^{\ddagger} = -13.6$ cm^3 mol^{-1} characterizing $[Be(H_2O)_4]^{2+}$ is the largest negative value observed for water exchange on a metal aqua ion which is consistent with the operation of an **A** mechanism and compares with $\Delta V^{\ddagger} = -12.9$ cm^3 mol^{-1} estimated for an **A** water-exchange mechanism.

On the basis of an **A** mechanism operating, the observed k_{H_2O} is a pseudo-first-order rate constant from which a second-order $k_{H_2O} = 13.2$ kg mol^{-1} s^{-1} may be calculated.

The larger r_M (=72 pm) of Mg^{2+} results in octahedral $[Mg(H_2O)_6]^{2+}$ for which water exchange is characterized by k_{H_2O} (298 K) = $6.7 \cdot 10^5$ s^{-1}, $\Delta H^{\ddagger} = 49.1$ kJ mol^{-1}, $\Delta S^{\ddagger} = +31.1$ J K^{-1} mol^{-1}, and $\Delta V^{\ddagger} = +6.7$ cm^3 mol^{-1}, consistent with the operation of either a **D** or an $\mathbf{I_d}$ mechanism [51]. There are few ligand-substitution data for $Mg(H_2O)_6]^{2+}$, but ultrasonic studies of substitution by SO_4^{2-} and CrO_4^{2-} are both characterized by $k_{23} = 1 \cdot 10^5$ s^{-1} (*Eqn. 3*) [28], which is comparable to k_{H_2O} when a statistical factor is taken into account. In the same study, $k_{23} = 2 \cdot 10^7$ s^{-1} was determined for the substitution of CrO_4^{2-} on $[Ca(H_2O)_6]^{2+}$, consistent with increasing lability towards water exchange and ligand substitution as r_M increases to 100 pm for Ca^{2+}.

The least labile of the main-group-metal aqua ions is $[Al(H_2O)_6]^{3+}$ (k_{H_2O} (298 K) = 1.29 s^{-1}, $\Delta H^{\ddagger} = 84.7$ kJ mol^{-1}, $\Delta S^{\ddagger} = +41.6$ J K^{-1} mol^{-1}, and $\Delta V^{\ddagger} = +5.7$ cm^3 mol^{-1}) as a consequence of its small r_M (=53.5 pm) and which undergoes water exchange through either an $\mathbf{I_d}$ or a **D** mechanism [43]. The high surface-charge density of Al^{3+} polarizes coordinated water such that protolysis readily occurs. This lowers the effective surface charge density of Al^{3+} and labilizes the five coordinated waters in $[Al(OH)(H_2O)_5]^{2+}$ by a factor of 10^4 (k_{H_2O} (298 K) = $3.1 \cdot 10^4$ s^{-1}, $\Delta H^{\ddagger} = 36.4$ kJ mol^{-1}, and $\Delta S^{\ddagger} = +36.4$ J K^{-1} mol^{-1} [52]). This substantial increase in lability coincides with observations that five hydroxamic acids ($R^1C(=O)N(R^2)OH$, where R^1 and R^2 are either H, alkyl or aryl groups) substitute on $[Al(OH)(H_2O)_5]^{2+}$ *ca.* 10^4 times faster than they do on $[Al(H_2O)_6]^{3+}$, where $k_{23}K_{12}$ (298 K) (*Eqn. 4*) shows a small range of 2300 to 2600 dm^3 mol^{-1} s^{-1} [36]. The same hydroxamic acids substitute on $[Al(H_2O)_6]^{3+}$ with $k_{23}K_{12}$ (298 K) in the range 0.15–0.23 dm^3 mol^{-1} s^{-1} from which $k_{23}' = 2.0-3.1$ s^{-1} may be estimated on the basis that $k_{23}K_{12} = k_{23}'SK_{12}$ where the statistical factor $S = 0.75$ and $K_{12} \approx 0.1$ dm^3 mol^{-1}, and it is assumed that $k_{23}' \approx k_{H_2O}$ for a **d**-activated mechanism. This calculation and the small variation of $k_{23}K_{12}$ for both $[Al(H_2O)_6]^{3+}$ and $[Al(OH)(H_2O)_5]^{2+}$ are consistent with the operation of **d**-activated ligand-substitution mechanisms in both cases. (The S and K_{12} values employed in such calculations have a major effect on the magnitude of the derived k_{23}', and variations in these may account for reported k_{23}' values varying by up to an order of magnitude on either side of k_{H_2O} for other ligand substitutions on $[Al(H_2O)_6]^{3+}$.) In contrast, for $[Fe(H_2O)_6]^{3+}$, the same hydroxamic acids substitute with $k_{23}K_{12}$ (298 K) = 1–4.4 dm^3 mol^{-1} s^{-1} [53], which gives $k_{23}' = 13-57$ (assuming $S = 0.75$ and $K_{12} \approx 0.1$ dm^3 mol^{-1}) which are smaller than the experimental k_{H_2O} (298 K) = $1.6 \cdot 10^2$ s^{-1} [54][55]. This, together with the 4.4-fold variation of $k_{23}K_{12}$, indicates the operation of an **a**-activated ligand-substitution mechanism for $[Fe(H_2O)_6]^{3+}$ in common with the $\mathbf{I_a}$ mechanism assigned to it for water exchange.

An $\mathbf{I_d}$ or a **D** mechanism operates for $[Ga(H_2O)_6]^{3+}$ (k_{H_2O} (298 K) = $4.0 \cdot 10^2$ s^{-1}, $\Delta H^{\ddagger} = 67.1$ kJ mol^{-1}, $\Delta S^{\ddagger} = +30.1$ J K^{-1} mol^{-1}, and $\Delta V^{\ddagger} = +5.0$ cm^3 mol^{-1} [44]), which is more labile than its Al^{3+} analogue because of its larger r_M (=62 pm). This is also the case for $[Ga(OH)(H_2O)_5]^{2+}$ (k_{H_2O} (298 K) = $(0.6-2.0) \cdot 10^5$ s^{-1}, $\Delta H^{\ddagger} = 58.9$ kJ mol^{-1}, and $\Delta V^{\ddagger} = +6.2$ cm^3 mol^{-1}), which is greatly labilized towards water exchange by comparison with $[Ga(H_2O)_6]^{3+}$. Substantial variations occur in the k_{23}' values estimated for ligand substitution on $[Ga(H_2O)_6]^{3+}$, probably due to their sensitivity to the S and K_{12} values used [56]. (However, the substitution of uncharged tropolone (=2-

hydroxycyclohepta-2,4,6-trien-1-one) on $[Ga(H_2O))_6]^{3+}$ is characterized by $\Delta V^{\ddagger} = +4.0$ cm^{3+} mol^{-1}, consistent with a **d**-activated mechanism operating [57].) Although theoretical considerations indicate that an **a**-activated water-exchange mechanism operates for $[In(H_2O)_6]^{3+}$ [42], no experimental data is available for $[In(H_2O)_6]^{3+}$ as is also the case for $[Tl(H_2O)_6]^{3+}$. Generally, the variations in derived k_{23}' values for $[Al(H_2O)_6]^{3+}$ and $[Ga(H_2O))_6]^{3+}$ are smaller than those reported for $[Cr(H_2O))_6]^{3+}$ and $[Fe(H_2O)_6]^{3+}$, where **a**-activated mechanisms operate as is discussed in *Sect. 12* [54][58].

8. Water Exchange on the Transition-Metal Aqua Ions. – The lability of the divalent first-row-transition-metal aqua ions generally increases in the sequence $V^{2+} < Ni^{2+} < Co^{2+} \approx Fe^{2+} < Mn^{2+} \approx Zn^{2+} < Cu^{2+} \approx Cr^{2+}$ (*Fig. 1* and *Table 1* [59–62]), which reflects the different electronic occupancy of their *d*-orbitals. This variation in lability is qualitatively in accord with the expectations arising from ligand-field activation energies (LFAEs) calculated for **a**- and **d**-activated mechanisms for the first six metal aqua ions as is also the case for the trivalent metal aqua ions with similar electronic configurations [20–22]. Large LFAEs contribute to the $\Delta H^{\ddagger}$ of the high-spin d^3-and d^8-metal aqua ions causing $[V(H_2O)_6]^{2+}$, $[Ni(H_2O)_6]^{2+}$, and $[Cr(H_2O)_6]^{3+}$ to be much less labile than the other di- and trivalent first-row-transition-metal aqua ions. (Similar conclusions are drawn from molecular-orbital calculations [63].) The change from **a**- to **d**-activation as the occupancy of the d-orbitals increases may be qualitatively explained through an increasing repulsion between an entering H_2O molecule approaching an octahedral face of $[M(H_2O)_6]^{2+/3+}$ and electrons in the t_{2g} orbitals disfavoring the increased coordination number required in an **a**-transition state, so that a **d**-transition state is favored as d-orbital occupancy increases. Similarly, it is expected that, as the antibonding e_g orbitals fill, a **d**-activation mode will be favored. *Ab initio* calculations for water exchange on the d^0 to d^{10} six-coordinate first-row-transition-metal ions predict also this change from **a**- to **d**-activation, so that only **A** mechanisms are possible for $[Sc(H_2O)_6]^{3+}$ and its Ti^{3+} and V^{3+} analogues, only **D** mechanisms are possible for $[Ni(H_2O)_6]^{2+}$ and its Cu^{2+} and Zn^{2+} analogues, while a gradual change from **a**- to **d**-activation is predicted for other first-row-transition-metal aqua ions with d^2 to d^7 electronic configurations [64–66]. Density-function calculations also indicate that water exchange on $[Zn(H_2O)_6]^{2+}$ is likely to occur through a **D** mechanism [67]. (The high lability of $[Cu(H_2O)_6]^{2+}$ and $[Cr(H_2O)_6]^{2+}$ seemingly arise from stereochemical effects reflecting their d^9 and d^4 electronic configurations as is discussed in *Sect. 9.*) However, the effect of d-orbital occupancy is not quite so clear cut for second- and third-row-transition-metal aqua ions. While quantum-mechanical calculations including second-coordination-sphere hydration show that for t_{2g}^6 $[Ru(H_2O)_6]^{2+}$, a **D** or $\mathbf{I_d}$ mechanism operates for water exchange as expected from the above predictions, such is not the case for t_{2g}^6 $[Rh(H_2O)_6]^{3+}$ and t_{2g}^6 $[Ir(H_2O)_6]^{3+}$ for which $\mathbf{I_a}$ water-exchange mechanisms operate, in agreement with experimental data [45][46]. The difference appears to arise from the stronger $M^{3+}-OH_2$ bonds of the trivalent metal aqua ions.

9. Six-Coordinate Divalent Transition-Metal Aqua Ions. – The deduction of water-exchange mechanisms of the divalent first-row-transition-metal aqua ions rests on the sign and magnitude of their $\Delta V^{\ddagger}$ (*Table 1*). None of the $\Delta V^{\ddagger}$ values approach the -13.5

Table 1. *Parameters for Water Exchange on Transition-Metal Ions*

$[M(H_2O)_n]^{m+}$	r_M a))/pm	d-Electron config.	k_{H_2O} (298 K) b))/s^{-1}	$\Delta H^‡$/kJ mol^{-1}	$\Delta S^‡$/J K^{-1} mol^{-1}	$\Delta V^‡$/cm^3 mol^{-1}	Mechanism
$[V(H_2O)_6]^{2+}$	79	t_{2g}^3	$8.7 \cdot 10^{1}$ c))	61.8	− 0.4	− 4.1	$\mathbf{I_a}$
$[Mn(H_2O)_6]^{2+}$	83	$t_{2g}^3e^2$	$2.1 \cdot 10^{7}$ d))	32.9	+ 5.7	− 5.4	$\mathbf{I_a}$
$[Fe(H_2O)_6]^{2+}$	78	$t_{2g}{}^4e_g{}^2$	$4.4 \cdot 10^{6}$ d))	41.4	+ 21.2	+ 3.8	$\mathbf{I_d}$
$[Co(H_2O)_6]^{2+}$	74.5	$t_{2g}^5e_g{}^2$	$3.2 \cdot 10^{6}$ d))	46.9	+ 37.2	+ 6.1	$\mathbf{I_d}$
$[Ni(H_2O)_6]^{2+}$	69	$t_{2g}^6e_g{}^2$	$3.15 \cdot 10^{4}$ d))	56.9	+ 32.0	+ 7.2	$\mathbf{I_d}$
$[Cu(H_2O)_6]^{2+}$	73	d^9	$4.4 \cdot 10^{9}$ e))	11.5	− 21.8	+ 2.0	$\mathbf{I_d}$
$[Cu(H_2O)_5]^{2+}$		d^9	$5.7 \cdot 10^{9}$ f))				
$[Ru(H_2O)_6]^{2+}$	73 g))	t_{2g}^6	$1.8 \cdot 10^{-2}$ g))	87.8	+ 16.1	− 0.4	$\mathbf{I_d}$
$[Pd(H_2O)_4]^{2+}$	64	d^8	$5.6 \cdot 10^{2}$ h))	49.5	− 26	− 2.2	$\mathbf{I_a}$
			$1.0 \cdot 10^{1}$ h)) i))	49.5	− 60.1	− 2.2	$\mathbf{I_a}$
$[Pt(H_2O)_4]^{2+}$	60	d^8	$3.9 \cdot 10^{-4}$ j))	89.7	− 9	− 4.6	$\mathbf{I_a}$
			$7.1 \cdot 10^{-6}$ j)) i))		− 43	− 4.6	$\mathbf{I_a}$
$[Ti(H_2O)_6]^{3+}$	67	$t_{2g}{}^1$	$1.8 \cdot 10^{5}$ k))	43.4	+ 1.2	− 12.1	**A**, $\mathbf{I_a}$
$[V(H_2O)_6]^{3+}$	64	t_{2g}^2	$5.0 \cdot 10^{2}$ l))	49.4	− 27.8	− 8.9	$\mathbf{I_a}$
$[Cr(H_2O)_6]^{3+}$	61.5	t_{2g}^3	$2.4 \cdot 10^{-6}$ m))	108.6	+ 11.6	− 9.6	$\mathbf{I_a}$
$[Cr(H_2O)_5(OH)]^{2+}$			$1.8 \cdot 10^{-4}$ m))	111.0	+ 55.6	+ 2.7	$\mathbf{I_a}$
$[Fe(H_2O)_6]^{3+}$	64.5	$t_{2g}^3e_g{}^2$	$1.6 \cdot 10^{2}$ n)) o))	64.0	+ 12.1	− 5.4	$\mathbf{I_a}$
$[Fe(H_2O)_5(OH)]^{2+}$			$1.2 \cdot 10^{5}$ i)) n)) o))	42.4	+ 5.3	+ 7.0	$\mathbf{I_d}$
$[Ru(H_2O)_6]^{3+}$	68	t_{2g}^5	$3.5 \cdot 10^{-6}$ p))	89.8	− 48.3	− 8.3	$\mathbf{I_a}$
$[Ru(H_2O)_5(OH)]^{2+}$			$5.9 \cdot 10^{-4}$ p))	95.8	+ 14.9	+ 0.9	**I**
$[Rh(H_2O)_6]^{3+}$	66.5	t_{2g}^6	$2.2 \cdot 10^{-9}$ q))	131	+ 29	− 4.2	$\mathbf{I_a}$
$[Rh(H_2O)_5(OH)]^{2+}$			$4.2 \cdot 10^{-5}$ q))	103	–	+ 1.5	**I**
$[Ir(H_2O)_6]^{3+}$	68	t_{2g}^6	$1.1 \cdot 10^{-10}$ r))	130.5	+ 2.1	− 5.7	$\mathbf{I_a}$
$[Ir(H_2O)_5(OH)]^{2+}$			$5.6 \cdot 10^{-7}$ r))			+ 1.3	**I**

a) [18]. b) Rate constant for the exchange of a particular H_2O molecule. c) [59]. d) [60]. e) [61]. f) [62]. g) [47]. h) [87]. i) dm^3 mol^{-1} s^{-1}. j) [88]. k) [92]. l) [91]. m) [58]. n) [54]. o) [55]. p) [47]. q) [48]. r) [17].

and $+13.5$ cm^3 mol^{-1} anticipated for **A** and **D** mechanisms, respectively, on the basis of the *Swaddle* model [38]. Accordingly, $\mathbf{I_a}$ and $\mathbf{I_d}$ mechanisms are assigned when $\Delta V^{\ddagger}$ is negative and positive, respectively, for $[V(H_2O)_6]^{2+}$ to $[Ni(H_2O)_6]^{2+}$ [59][60]. The increased lability of d^9 $[Cu(H_2O)_6]^{2+}$ has been interpreted through two models. The first invokes a dynamic *Jahn–Teller* effect through which a tetragonal distortion randomly and very rapidly reorientates two elongated and weaker Cu$-$OH$_2$ bonds along the x, y, and z axes so that the lifetime of a given distortion, $5.1 \cdot 10^{-12}$ s, is much less than τ_{H_2O} (298 K) $= 2.3 \cdot 10^{-10}$ s [61]. Thus, each H$_2$O molecule in $[Cu(H_2O)_6]^{2+}$ is labilized as it experiences 45 reorientations which include several elongations of the Cu$-$OH$_2$ bond before exchanging. An alternative model is based on neutron diffraction and first-principals-molecular-dynamics studies and explains the labilization toward water exchange through five-coordinate $[Cu(H_2O)_5]^{2+}$ rapidly interconverting between square-pyramidal and trigonal-bipyramidal configurations and τ_{H_2O} (298 K) $= 1.9 \cdot 10^{-10}$ s [62]. The small $\Delta V^{\ddagger} = +2.0$ cm^3 mol^{-1} is consistent with the operation of an $\mathbf{I_d}$ mechanism. As d^4 $[Cr(H_2O)_6]^{2+}$ experiences *Jahn–Teller* effects similar to those of a d^9 system, labilizing effects similar to those experienced by $[Cu(H_2O)_6]^{2+}/[Cu(H_2O)_5]^{2+}$ are anticipated, but no direct data for water exchange on $[Cr(H_2O)_6]^{2+}$ are available.

Ligand-substitution rates on $[Fe(H_2O)_6]^{2+}$ to $[Zn(H_2O)_6]^{2+}$ show little variation with the nature of the substituting ligand as anticipated for metal aqua ions for which $\mathbf{I_d}$ water-exchange mechanisms operate [12][68–75]. However, the small amount of ligand-substitution data for $[V(H_2O)_6]^{2+}$ and $[Mn(H_2O)_6]^{2+}$, which undergo water exchange through an $\mathbf{I_a}$ mechanism, also show little discrimination by the entering ligand. This may reflect the borderline hard-acid nature of V^{2+} and Mn^{2+} that restricts substituting ligands to hard bases, and thereby limits the variation of nucleophilicity to too small a range for a substitution-rate dependence on the entering ligand to be detected. Nevertheless, the negative $\Delta V^{\ddagger}$ values for ligand substitution on $[V(H_2O)_6]^{2+}$ and $[Mn(H_2O)_6]^{2+}$, and the positive values for $[Fe(H_2O)_6]^{2+}$ to $[Ni(H_2O)_6]^{2+}$ correlate well with those for water exchange [71–75].

The effect of descending a group and the corresponding increase in r_M is shown for 2,2′-bipyridine substitution on $[Zn(H_2O)_6]^{2+}$ ($r_M = 74$ pm) and the reverse reaction for which $\Delta V^{\ddagger} = +7.1$ and $+3.6$ cm^3 mol^{-1}, respectively, characterizing $\mathbf{I_d}$ mechanisms [76]. In contrast, $\Delta V^{\ddagger} = -5.5$ and -6.9 cm^3 mol^{-1} for 2,2′-bipyridine substitution on $[Cd(H_2O)_6]^{2+}$ for which the operation of an $\mathbf{I_a}$ mechanism is favored as a result of an increased r_M ($= 95$ pm). Another effect of descending a group is a change in electronic configuration which can have profound effects. This is exemplified by high-spin $t_{2g}{}^4e_g{}^2$ $[Fe(H_2O)_6]^{2+}$ ($r_M = 78$ pm) [60], which undergoes water exchange through an $\mathbf{I_d}$ mechanism (assigned on the basis of $\Delta V^{\ddagger} = +3.8$ cm^3 mol^{-1}) and is *ca.* 10^8 more labile than low-spin t^6_{2g} $[Ru(H_2O)_6]^{2+}$ because of the latter's greater LFAE and smaller r_M ($= 73$ pm) reflected in a much larger $\Delta H^{\ddagger}$ and the operation of an **I** mechanism as assigned from $\Delta V^{\ddagger} = -0.4$ cm^3 mol^{-1}, respectively [47]. However, quantum-mechanical calculations [45] show that volume contraction in the transition state due to shortening of the Ru$^{2+}-$OH$_2$ distance is -1.7 cm^3 mol^{-1}, consistent with a volume increase of *ca.* $+1.3$ cm^3 mol^{-1} arising from bond breaking in an $\mathbf{I_d}$ mechanism by the leaving H$_2$O molecule and $\Delta V^{\ddagger} = -0.4$ cm^3 mol^{-1} as discussed in *Sect. 6*. Accordingly, ligand substitution by a wide range of ligands on $[Ru(H_2O)_6]^{2+}$ is independent of the nature of the substituting ligand [77][78].

10. The Effect of Other Ligands on Water Lability in Divalent Transition-Metal Aqua Ions. – The entry of another ligand into the first coordination sphere of $[M(H_2O)_n]^{m+}$ modifies the effective surface-charge density of M^{m+}, the LFAE, and the stereochemistry to an extent depending on the nature of the entering ligand and M^{m+}, and this may alter the lability of the remaining H_2O molecules. The effect of protolysis to give the labilizing hydroxo ligand has already been noted in *Sect. 7* and is further discussed in *Sect. 12*. Other ligands in the first coordination sphere can also cause substantial labilization as shown for *mer*- and *fac*-$[Ni(NH_3)_3(H_2O)_3]^{2+}$ where k_{H_2O} (298 K) $= 2.5 \cdot 10^5$, $6.1 \cdot 10^5$, and $2.5 \cdot 10^6$ s^{-1}, compared with k_{H_2O} (298 K) $= 3.15 \cdot 10^4$ s^{-1} for $[Ni(H_2O)_6]^{2+}$, through greater σ-donation to the Ni^{2+} center [79]. Similarly, 2,2′,2″-nitrilotriethylamine (tren = *N*,*N*-bis(2-aminoethyl)ethane-1,2-diamine) in $[Ni(tren)(H_2O)_2]^{2+}$ labilizes the two inequivalent H_2O (k_{H_2O} (298 K) $= 8.2 \cdot 10^5$ and $9.0 \cdot 10^6$ s^{-1} [80]) as does 1,4,7,10-tetraazacyclododecane (cyclen) the two equivalent H_2O molecules in $[Ni(cyclen)(H_2O)_2]^{2+}$ (k_{H_2O} (298 K) $= 2.1 \cdot 10^7$ s^{-1} [81]). A very different type of ligand, π-bonding benzene, greatly labilizes H_2O in $[Ru(\eta^6\text{-}C_6H_6)(H_2O)_3]^{2+}$ (k_{H_2O} (298 K) = 11.5 s^{-1}, $\Delta H^{\ddagger} = 75.9$ kJ mol^{-1}, $\Delta S^{\ddagger} = +29.9$ J K^{-1} mol^{-1}, $\Delta V^{\ddagger} = +1.5$ cm^3 mol^{-1}) by comparison with that in $[Ru(H_2O)_6]^{2+}$ (k_{H_2O} (298 K) $= 1.8 \cdot 10^{-2}$ s^{-1}), largely as a consequence of a decrease in $\Delta H^{\ddagger}$ [82]. However, coordinated H_2O is not invariably labilized by the entry of another ligand into the first coordination sphere as shown by 2,2′-bipyridine and 2,2′,2″-terpyridine which cause only minor changes in lability, probably because their σ-donation of electron density to M^{m+} is offset by π-bonding-electron-density withdrawal [83]. Sometimes, other ligands may decrease H_2O lability as does trimethyl phosphate and 3-(2-pyridyl)-5,6-bis(4-phenylsulfonic acid)-1,2,4-triazine (=4,4′-[3-(pyridin-2-yl)-1,2,4-triazine-5,6-diyl]bis[benzenesulfonic acid) when coordinated to Cu^{2+}, possibly because of a decrease in coordination number [84].

11. Divalent Square-Planar Transition-Metal Aqua Ions. – While d^8 Rh^+, Ir^+, Ni^{2+}, Pd^{2+}, Pt^{2+}, and Au^{3+} all form square-planar complexes because of favorable ligand-field effects, those of Pd^{2+} and Pt^{2+} have dominated ligand-substitution studies [85], which have been given a particular impetus because of the importance of the Pt^{2+} anticancer drugs [86]. In the absence of large steric-crowding effects, ligand substitutions on Pd^{2+} and Pt^{2+} are most readily explained by the entering ligand making a nucleophilic attack from above the square plane to form a square-pyramidal intermediate, which, through a progression of square-pyramidal and trigonal-bipyramidal transition states and intermediates, displaces the leaving ligand with retention of configuration. It is reasonable to assume that $[Pd(H_2O)_4]^{2+}$ and $[Pt(H_2O)_4]^{2+}$ undergo water exchange through a similar mechanistic sequence. This reaction path has been attributed to the 16-electron valence-shell Pd^{2+} and Pt^{2+} center achieving the noble-gas 18-electron configuration.

Mainly as a result of a smaller $\Delta H^{\ddagger}$ (*Table 1*), k_{H_2O} for $[Pd(H_2O)_4]^{2+}$ is $1.4 \cdot 10^6$ greater than that for $[Pt(H_2O)_4]^{2+}$, and for both metal aqua ions, the small negative $\Delta V^{\ddagger}$ values are consistent with **a**-activated mechanisms operating [87][88]. It is likely that a very weakly interacting H_2O lies close to the metal center on either side of the square plane of both metal aqua ions in the ground state and that $\Delta V^{\ddagger}$ for the formation of the five-coordinate transition state is minimized as a result. Consistent with this, density-function calculations show **a**-activation to be energetically favored over **d**-activation for both $[Pd(H_2O)_4]^{2+}$ and $[Pt(H_2O)_4]^{2+}$ [89]. Ligand-substitution studies show $[Pt(H_2O)_4]^{2+}$ to be more sensitive to the nature of the entering ligand X^{x-} than is $[Pd(H_2O)_4]^{2+}$, consistent with Pt^{2+} being a softer *Lewis* acid than Pd^{2+}. This is illustrated by the observed ligand-substitution rate constant k_{23}, for $[Pd(H_2O)_4]^{2+}$ being $1.83 \cdot 10^4$ and $1.14 \cdot 10^6$ dm^3 mol^{-1} s^{-1} for $X^{x-} = Cl^-$ and I^-, respectively, and $2.66 \cdot 10^{-2}$ and 7.7 dm^3 mol^{-1} s^{-1} for $[Pd(H_2O)_4]^{2+}$ [90]. In each case, k_{23} for Cl^- is much greater than $4k_{H_2O}$ for water exchange (40.8 and $2.8 \cdot 10^{-5}$ dm^3 mol^{-1} s^{-1} for $[Pd(H_2O)_4]^{2+}$ and $[Pt(H_2O)_4]^{2+}$, resp.), consistent with the operation of an **a**-activated ligand-substitution mechanism.

12. Six-Coordinate Trivalent Transition-Metal Aqua Ions. – The order of lability increases in the sequence $[Cr(H_2O)_6]^{3+} \ll [Fe(H_2O)_6]^{3+} \leq [V(H_2O)_6]^{3+} \ll [Ti(H_2O)_6]^{3+}$ as LFAE contributions to $\Delta H^{\ddagger}$ decrease (*Table* 1) [54][55][58][59][91][92]. The negative $\Delta V^{\ddagger}$ values characterizing all four metal aqua ions are consistent with **a**-activation modes for water exchange, and that for $[Ti(H_2O)_6]^{3+}$ ($\Delta V^{\ddagger} = -12.1$ cm^3 mol^{-1}) approaches $\Delta V^{\ddagger} = -13.5$ cm^3 mol^{-1} calculated for an **A** mechanism by *Swaddle* [39]. The influence of d electronic configuration on lability is well-illustrated by t_{2g}^2 $[V(H_2O)_6]^{3+}$ being 5.7 times more-labile than t_{2g}^3 $[V(H_2O)_6]^{2+}$ [59] because of the larger LFAE of the latter species despite the lesser surface-charge density of the V^{2+} center. This influence is also shown by low-spin t_{2g}^5 $[Ru(H_2O)_6]^{3+}$ and t_{2g}^6 $[Rh(H_2O)_6]^{3+}$ with the large LFAE of the latter causing it to be three orders of magnitude less labile than the former, mainly as a consequence of its greater $\Delta H^{\ddagger}$ [47]. A large LFAE, and consequently large $\Delta H^{\ddagger}$, also accounts for the remarkable inertness of t_{2g}^6 $[Ir(H_2O)_6]^{3+}$ [17].

The charge of M^{3+} polarizes coordinated water in $[M(H_2O)_6]^{3+}$ such that protolysis produces $[M(H_2O)_5(OH)]^{2+}$, and the overall rate law for water exchange is given by *Eqn. 8* in which k_{H_2O} and k_{H_2O}'' characterize the exchange of a particular H_2O molecule on $[M(H_2O)_6]^{3+}$ and $[M(H_2O)_5(OH)]^{2+}$, respectively. Water lability is greatly increased in $[M(H_2O)_5(OH)]^{2+}$ with $\Delta V_{H_2O}''^{\ddagger}$ values being large and positive when $M^{3+} = Fe^{3+}$, consistent with an $\mathbf{I_d}$ mechanism operating, and small and positive when $M^{3+} = Cr^{3+}$, Ru^{3+}, Rh^{3+}, and Ir^{3+}, consistent with an **I** mechanism operating. The substantial σ-electron-donating power of the hydroxo ligand strengthens the $M^{3+}-OH$ bond while weakening the $M^{3+}-OH_2$ bonds. This labilizes H_2O in $[M(H_2O)_5(OH)]^{2+}$ and favors a change towards **d**-activation. This labilization is greater for the lighter $[M(H_2O)_5(OH)]^{2+}$ of the same d electronic configuration as shown by $M^{3+} = d^5$ Fe^{3+}, d^5 Ru^{3+}, d^6 Rh^{3+}, and d^6 Ir^3 (*Table 1*) consistent with the greater electron population of the heavier M^{3+} diminishing the effect of σ-electron donation by the hydroxo ligand.

$$k_{H_2O(obs)} = k_{H_2O} + k_{H_2O}'/[H^+] = k_{H_2O} + k_{H_2O}''K_a/[H^+] \qquad (8)$$

Ligand substitution on $[M(H_2O)_6]^{3+}$ and $[M(H_2O)_5(OH)]^{2+}$ is characterized by a two-term rate law similar to *Eqn. 8*, and generally the activation modes for ligand substitution and water exchange are the same [12]. Thus, for $[Ti(H_2O)_6]^{3+}$, the substitution rate increases 225-fold with the basicity of the substituting monoanionic X^-, consistent with substitution on $[Ti(H_2O)_6]^{3+}$ occurring through an **A** mechanism as is the case for water exchange [92][93]. Similarly, both ligand substitution and water exchange on $[V(H_2O)_6]^{3+}$ occur through **a**-activated mechanisms [91][94–96]. Monoanionic ligand substitutions on $[Fe(H_2O)_6]^{3+}$ and $[Fe(H_2O)_5(OH)]^{2+}$, respectively, show 938- and 15-fold substitution-rate variations, respectively, consistent with the ligand-substitution mechanisms being the same as their $\mathbf{I_a}$ and $\mathbf{I_d}$ water-exchange mechanisms [12][54]. In a similar way, 2050- and 21-fold substitution-rate variations indicate that $\mathbf{I_a}$ and $\mathbf{I_d}$ mechanisms operate for $[Cr(H_2O)_6]^{3+}$ and $[Cr(H_2O)_5(OH)]^{2+}$, respectively [12][58]. While no water-exchange data is available for second-row t_{2g}^3 $[Mo(H_2O)_6]^{3+}$, ligand-substitution studies show it to be *ca.* 10^5 times more labile than $[Cr(H_2O)_6]^{3+}$ and to exhibit a ligand-substitution-rate variation consistent with the operation of an $\mathbf{I_a}$ substitution mechanism [97]. This is in accord with $\Delta V^{\ddagger} \approx -17$ cm^3 mol^{-1} for substitution by NCS$^-$ [98]. Although a greater LFAE is anticipated for $[Mo(H_2O)_6]^{3+}$ by comparison with that of $[Cr(H_2O)_6]^{3+}$, its greater lability may be a consequence of a greater extent of bond making in the transition state. Other second- and third-row-metal aqua ions have also caused some uncertainty in mechanistic discussion as exemplified by t_{2g}^6 $[Rh(H_2O)_6]^{3+}$ and $[Ir(H_2O)_6]^{3+}$ to which $\mathbf{I_a}$ mechanisms for water exchange were assigned on the basis of $\Delta V^{\ddagger} = -4.2$ and -5.7 cm^3 mol^{-1}, respectively. In contrast, the similarity of the substitution rates for Cl$^-$ and Br$^-$ on $[Rh(H_2O)_6]^{3+}$ has been cited as evidence for the operation of a **D** ligand substitution [99]. However, this conclusion has been challenged by *Richens* and co-workers, who find Br$^-$ substitution on $[Rh(H_2O)_6]^{3+}$ to occur through an $\mathbf{I_a}$ mechanism [100].

13. The Effect of Other Ligands on Water Lability in Trivalent Transition-Metal Aqua Ions. – Mainly one- to five-NH$_3$ substituted Cr^{3+} complexes have provided k_{H_2O} (298 K) ranging from $4.49 \cdot 10^{-6}$ s^{-1} for $[Cr(NH_3)(H_2O)_5]^{3+}$ to $5.8 \cdot 10^{-5}$ s^{-1} ($\Delta H^{\ddagger} =$ 97.1 kJ mol^{-1}, $\Delta S^{\ddagger} = 0$ K^{-1} mol^{-1}, $\Delta V^{\ddagger} = -5.8$ cm^3 mol^{-1}) for $[Cr(NH_3)_5(H_2O)]^{3+}$ showing quite a small influence on H$_2$O lability [101–103]. Analogous Co^{3+} complexes with fewer than either four NH$_3$ ligands or four amine donor groups are unstable, and k_{H_2O} (298 K) ranging from $5.7 \cdot 10^{-6}$ s^{-1} ($\Delta H^{\ddagger} = 111.3$ kJ mol^{-1}, $\Delta S^{\ddagger} = +28$ J K^{-1} mol^{-1}, $\Delta V^{\ddagger} = +1.2$ cm^3 mol^{-1}) for $[Co(NH_3)_5(H_2O)]^{3+}$ to $2 \cdot 10^{-4}$ s^{-1} for $[Co(cyclen)(H_2O)_2]^{3+}$ have been reported [8][104] (cyclen = 1,4,7,10-tetraazacyclodecane). When steric crowding is increased in the penta(methylamine) complexes, $[Cr(CH_3NH_2)_5(H_2O)_5]^{3+}$ (k_{H_2O} (298 K) $= 4.1 \cdot 10^{-6}$ s^{-1}, $\Delta H^{\ddagger} = 98.5$ kJ mol^{-1}, $\Delta S^{\ddagger} = -17.5$ J K^{-1} mol^{-1}, $\Delta V^{\ddagger} =$ -3.8 cm^3 mol^{-1}) shows a decrease in lability by comparison with $[Cr(NH_3)_5(H_2O)]^{3+}$, whereas $[Co(CH_3NH_2)_5(H_2O)_5]^{3+}$ (k_{H_2O} (298 K) $= 7.0 \cdot 10^{-4}$ s^{-1}, $\Delta H^{\ddagger} = 99.0$ kJ mol^{-1}, $\Delta S^{\ddagger} = +26.7$ J K^{-1} mol^{-1}, $\Delta V^{\ddagger} = +5.7$ cm^3 mol^{-1}) shows an increase in lability by comparison with $[Co(NH_3)_5(H_2O)]^{3+}$, and their $\Delta V^{\ddagger}$ are consistent with $\mathbf{I_a}$ and $\mathbf{I_d}$ mechanisms, respectively [105]. These opposite changes in lability are the expected effects of steric crowding on lability for $\mathbf{I_a}$ and $\mathbf{I_d}$ mechanisms. The analogous pair of Rh^{3+} complexes $[Rh(NH_3)_5(H_2O)]^{3+}$ (k_{H_2O} (298 K) $= 8.4 \cdot 10^{-6}$ s^{-1}, $\Delta H^{\ddagger} = 103.0$ kJ mol^{-1}, $\Delta S^{\ddagger} = +3.3$ J K^{-1} mol^{-1}, $\Delta V^{\ddagger} = -4.1$ cm^3 mol^{-1}) and $[Rh(CH_3NH_2)_5(H_2O)]^{3+}$ (k_{H_2O} (298 K) $= 1.06 \cdot 10^{-5}$ s^{-1}, $\Delta H^{\ddagger} = 112.7$ kJ mol^{-1}, $\Delta S^{\ddagger} = +37.8$ J K^{-1} mol^{-1}, $\Delta V^{\ddagger} =$ $+1.2$ cm^3 mol^{-1}) show little change in lability, although their $\Delta V^{\ddagger}$ indicate a change from an $\mathbf{I_a}$ to an $\mathbf{I_d}$ mechanism, in accord with a decrease and an increase in **a**- and **d**-activation as steric crowding increases, respectively, as is also observed for the analogous Cr^{3+} and Co^{3+} pairs [105]. Both Rh^{3+} complexes are four orders of magnitude more labile than $[Rh(H_2O)_6]^{3+}$.

Despite the inertness of $[Rh(H_2O)_6]^{3+}$ and $[Ir(H_2O)_6]^{3+}$, the entry of the pentamethylcyclopentadienyl ligand $CpMe_5^-$ (=Cp*) into the first coordination sphere labilizes the three remaining H_2O ligands in $[Rh(\eta^5\text{-}Cp^*)(H_2O)_3]^{2+}$ (k_{H_2O} (298 K) = $1.6 \cdot 10^5$ s^{-1}, $\Delta H^\ddagger = 65.6$ kJ mol^{-1}, $\Delta S^\ddagger = +75.3$ J K^{-1} mol^{-1}, $\Delta V^\ddagger = +0.6$ cm^3 mol^{-1}) and $[Ir(\eta^5\text{-}Cp^*)(H_2O)_3]^{2+}$ (k_{H_2O} (298 K) = $2.5 \cdot 10^4$ s^{-1}, $\Delta H^\ddagger = 54.9$ kJ mol^{-1}, $\Delta S^\ddagger = +23.6$ J K^{-1} mol^{-1}, $\Delta V^\ddagger = +2.4$ cm^3 mol^{-1}) by factors of *ca.* 10^{14} [106]. This is largely a result of a halving of $\Delta H^\ddagger$ by comparison with those of the analogous hexaaqua ions which undergo water exchange through $\mathbf{I_a}$ mechanisms, and a change towards an $\mathbf{I_d}$ mechanism as shown by the positive $\Delta V^\ddagger$ values and also by ligand-substitution studies [107].

14. Transition-Metal Oxo Aqua Ions. – The best characterized of the monomeric first-row-transition-metal oxo aqua ions is $[VO(H_2O)_5]^{2+}$ in which the V^{4+} center lies above the plane defined by the four equatorial H_2O to which it is closer than to the axial H_2O. This difference in $V^{4+}-H_2O$ distances is consistent with exchange of the equatorial H_2O of $[VO(H_2O)_5]^{2+}$ (k_{H_2O} (298 K) = 500 s^{-1}, $\Delta H^\ddagger = 57.3$ kJ mol^{-1}, $\Delta S^\ddagger = -2.4$ J K^{-1} mol^{-1}, and $\Delta V^\ddagger = +1.9$ cm^3 mol^{-1}) occurring more slowly than the exchange of the axial H_2O (k_{H_2O} (298 K) $\approx 10^9$ s^{-1}) [108][109]. It appears that the k_{H_2O} (298 K) for direct water exchange at an equatorial site on $[VO(H_2O)_5]^{2+}$ is *ca.* 0.1 s^{-1}, and that the larger value of 500 s^{-1} arises from a rapid migration between the axial and equatorial sites characterized by $k_{\text{migration}} \approx 10^3$ s^{-1}. The oxo-ligand exchange is characterized by k_O (298 K) = $2.4 \cdot 10^{-5}$ s^{-1} [110], which is much slower than the exchange of the oxo ligand of $[TiO(H_2O)_5]^{2+}$ (k_O (298 K) = $1.6 \cdot 10^4$ s^{-1} [111]). The oxo ligand of the latter is thought to be more readily protonated and therefore labilized.

15. Trivalent Lanthanide Aqua Ions. – The trivalent lanthanide ions, Ln^{3+} (= La^{3+}, Ce^{3+}, Pr^{3+}, Nd^{3+}, Pm^{3+}, Sm^{3+}, Eu^{3+}, Gd^{3+}, Tb^{3+}, Dy^{3+}, Ho^{3+}, Er^{3+}, Tm^{3+}, Yb^{3+}, and Lu^{3+}) exhibit a smooth decrease in r_M from 121.6 to 103.2 pm for nine-coordinate La^{3+} to Lu^{3+} and from 116.0 to 97.7 pm for eight-coordinate La^{3+} to Lu^{3+} [18]. This lanthanide contraction arises from the sequential electronic filling of the 4f orbitals and increase in nuclear charge. Ligand-field effects are small because the 4f-electron cloud is diffuse, and substantial shielding is afforded by the 5s and 5p electrons. Generally, the Ln^{3+} behave as large low-surface-charge-density metal ions that vary their coordination numbers with change of ligand. For $[Ln(H_2O)_n]^{3+}$ in water, $n = 9$ for La^{3+} to Nd^{3+}, $n = 8$ for Gd^{3+} to Lu^{3+}, and an equilibrium exists between $[Ln(H_2O)_8]^{3+}$ and $[Ln(H_2O)_n]^{3+}$ for Pm^{3+} to Eu^{3+} [112–120]. The k_{H_2O} for water exchange on $[Gd(H_2O)_8]^{3+}$ to $[Lu(H_2O)_8]^{3+}$ decrease with decrease in r_M, and both $\Delta S^\ddagger$ and $\Delta V^\ddagger$ are negative. However, these $\Delta V^\ddagger$ are much less negative than either the $\Delta V^\ddagger = -12.9$ cm^3 mol^{-1} [39][121] calculated for either an **A** mechanism for water exchange or the volume change of -11 cm^3 mol^{-1} determined for $[Ce(H_2O)_8]^{3+}$ adding a H_2O molecule to form $[Ce(H_2O)_9]^{3+}$ [122], as is seen from *Table 2* [123–125]. Hence, an $\mathbf{I_a}$ mechanism is assigned to water exchange on these $[Ln(H_2O)_8]^{3+}$, and the decrease in k_{H_2O} and the increase in $\Delta H^\ddagger$ with decease in r_M is attributed to increasing steric crowding in the transition state. Attempts to directly determine k_{H_2O} (298 K) for $[Pr(H_2O)_9]^{3+}$ and $[Nd(H_2O)_9]^{3+}$ produced lower-limit estimates of $5 \cdot 10^8$ and $4 \cdot 10^8$ s^{-1}, respectively [126]. Overall, the directly determined k_{H_2O} data are consistent with the most-labile lanthanide centers being Pm^{3+}, Sm^{3+}, Eu^{3+}, and Gd^{3+}, for which the energies of

$[Ln(H_2O)_8]^{3+}$ and $[Ln(H_2O)_9]^{3+}$ are most similar and are in accord with ultrasonic studies, which show that sulfate substitution occurs most rapidly for Sm^{3+}, Eu^{3+}, and Gd^{3+} and decreases systematically as atomic number decreases or increases to either side of them [127].

Intuitively, the increase in coordination number of square-antiprismatic $[Ln(H_2O)_8]^{3+}$ to form a tricapped trigonal-prismatic $[Ln(H_2O)_9]^{3+}$ transition state is a reasonable stereochemical pathway for $\mathbf{I_a}$ water exchange on the smaller and heavier Ln^{3+} as the lighter and larger Ln^{3+} exist as either $[Ln(H_2O)_9]^{3+}$ or as an equilibrium mixture of $[Ln(H_2O)_8]^{3+}$ and $[Ln(H_2O)_9]^{3+}$ in water. It is also reasonable to assume that tricapped trigonal-prismatic $[Ln(H_2O)_9]^{3+}$ will proceed through a square-antiprismatic $[Ln(H_2O)_8]^{3+}$ $\mathbf{I_d}$ transition state for water exchange. This is in accord with Monte Carlo modelling, which predicts **a**- and **d**-activated water exchange on $[Ln(H_2O)_8]^{3+}$ and $[Ln(H_2O)_9]^{3+}$, respectively [128], and later molecular-dynamic simulations of water exchange on $[Nd(H_2O)_9]^{3+}$ and $[Yb(H_2O)_8]^{3+}$, which indicate the operation of $\mathbf{I_d}$ and $\mathbf{I_a}$ mechanisms, respectively [23–25]. It was also found that the equilibrium between $[Sm(H_2O)_9]^{3+}$ and $[Sm(H_2O)_8]^{3+}$ is maintained by a ninth H_2O molecule that exchanges rapidly between the first coordination sphere and the bulk in an alternation of addition and elimination reactions that does not readily fit into the **a**- and **d**-activation classifications [25].

Table 2. *Parameters for Water Exchange on Lanthanide Aqua Ions*

$[Ln(H_2O)_n]^{m+}$	r_M [a])/pm	$10^{-7}k_{H_2O}$ (298 K) [b])/s^{-1}	$\Delta H^{\ddagger}$/kJ mol^{-1}	$\Delta S^{\ddagger}$/J K^{-1} mol^{-1}	$\Delta V^{\ddagger}$/cm^3 mol^{-1}	Mechanism
$[Gd(H_2O)_8]^{3+}$	105.3	83.0 [c])	14.9	– 24.1	– 3.3	$\mathbf{I_a}$
$[Tb(H_2O)_8]^{3+}$	104.0	55.8 [d])[e])	12.1	– 36.9	– 5.7	$\mathbf{I_a}$
$[Dy(H_2O)_8]^{3+}$	102.7	43.4 [d])[e])	16.6	– 24.0	– 6.0	$\mathbf{I_a}$
$[Ho(H_2O)_8]^{3+}$	101.5	21.4 [d])[e])	16.4	– 30.5	– 6.6	$\mathbf{I_a}$
$[Er(H_2O)_8]^{3+}$	100.4	13.3 [d])[e])	18.4	– 27.8	– 6.9	$\mathbf{I_a}$
$[Tm(H_2O)_8]^{3+}$	99.4	9.1 [d])[e])	22.7	– 16.4	– 6.0	$\mathbf{I_a}$
$[Yb(H_2O)_8]^{3+}$	98.5	4.7 [d])[e])	23.3	– 21.0		

[a]) [19]. [b]) Rate constant for the exchange of a particular H_2O molecule. [c]) [123]. [d])[e]) [124][125].

An interesting effect of an oxidation-state change is afforded by a comparison between the very labile equilibrium between $[Eu(H_2O)_8]^{3+}$ and $[Eu(H_2O)_9]^{3+}$ and that between $[Eu(H_2O)_7]^{2+}$ and $[Eu(H_2O)_8]^{2+}$, where the latter is the minor species in the second equilibrium [18]. Although k_{H_2O} for water exchange in the first equilibrium has so far not been reported, it is reasonable to assume that the mechanism of water exchange on the two species is similar to that for its Sm^{3+} analogues. An extension of this argument to $[Eu(H_2O)_7]^{2+}$ (k_{H_2O} (298 K) $= 5.0 \cdot 10^9$ s^{-1}, $\Delta H^{\ddagger} = 15.7$ kJ mol^{-1}, $\Delta S^{\ddagger} = -7.0$ J K^{-1} mol^{-1}, and $\Delta V^{\ddagger} = -11.3$ cm^3 mol^{-1}) suggests a square-antiprismatic $[Eu(H_2O)_8]^{2+}$ transition state, and the large negative $\Delta V^{\ddagger}$ is consistent with the water-exchange process being close to the limiting **A** mechanism.

16. Water Exchange on Gd^{3+} Complexes and Practical Applications. – The complexing of Gd^{3+} by multidentate ligands can diminish the lability of water by several orders of magnitude in comparison with that of $[Gd(H_2O)_8]^{3+}$ [123][129] as illustrated by $[Gd(DOTA\text{-}4AmP)(H_2O)]^{5-}$, for which k_{H_2O} (298 K) $= 4 \cdot 10^4$ s^{-1} (*Fig. 4*)

[130]. This is further illustrated by water exchange on nine-coordinate $[Gd(DOTA)(H_2O)]^-$ (k_{H_2O} (298 K) = $4.8 \cdot 10^6$ s^{-1}, $\Delta H^\ddagger = 48.8$ kJ mol^{-1}, $\Delta S^\ddagger = +46.6$ J K^{-1} mol^{-1}, and $\Delta V^\ddagger = +10.5$ cm^3 mol^{-1} [123]) and eight-coordinate $[Gd\{TREN\text{-}bis(6\text{-}Me\text{-}HOPO)\text{-}(TAM\text{-}TRI)\}(H_2O)_2]$ (k_{H_2O} (298 K) = $5.3 \cdot 10^7$ s^{-1}, $\Delta H^\ddagger = 25.9$ kJ mol^{-1}, and $\Delta V^\ddagger = -5$ cm^3 mol^{-1} [131]) shown in *Fig. 4*. The decrease in lability is considered to arise largely from the rigidity introduced into the first coordination sphere. Thus, for $[Gd(DOTA)(H_2O)]^-$, the rigidity of DOTA greatly restricts flexing in the transition state and the participation of an incoming H_2O molecule, with the consequence that an

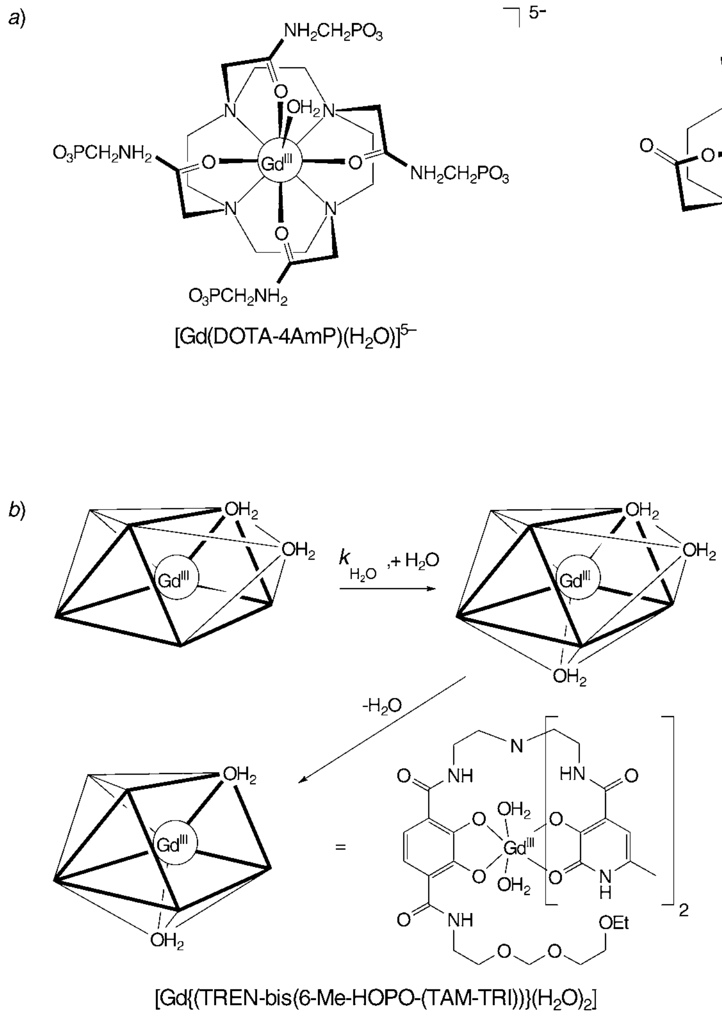

Fig. 4. a) *Structures of $[Gd(DOTA\text{-}4AmP)(H_2O)]^{5-}$ and $[Gd(DOTA)(H_2O)]^-$ in their* M *isomeric forms where the multidentate-ligand donor groups define a square antiprism* (the alternative *m* isomer has a twisted square-antiprismatic structure in which the side arms are rotated) *and* b) *water exchange on $[Gd\{TREN\text{-}bis(6\text{-}Me\text{-}HOPO)\text{-}(TAM\text{-}TRI)\}(H_2O)_2]$*

$\mathbf{I_d}$ mechanism operates and an increased $\Delta H^{\ddagger}$ diminishes lability. Similar effects apply to [Gd{TREN-bis(6-Me-HOPO)-(TAM-TRI)}$(H_2O)_2$], but there is sufficient flexibility to increase the coordination number to nine in an $\mathbf{I_a}$ transition state, and its lability is diminished less.

Apart from its intrinsic interest, $[Gd(DOTA)(H_2O)]^-$ is an important contrast agent used in magnetic-resonance imaging (MRI). The contrasting agent relaxes water protons by through-space dipole-dipole interactions between the unpaired electron spin of Gd^{3+} and the extracellular water protons so that they may be more readily distinguished from those of intracellular water and the image resolution enhanced. This relaxation is most effective for the protons of coordinated water, which is transmitted to bulk water through the water-exchange process, and the overall effectiveness of the extracellular proton relaxation is additionally dependent on the unpaired-electron relaxation times and the rate at which water in the second coordination sphere diffuses into bulk water [129][132]. It is essential that the MRI Gd^{3+} complex must be extremely stable to minimize toxicity due to $[Gd(H_2O)_8]^{3+}$, while at the same time possessing a k_{H_2O} and tumbling time to maximize water proton relaxation.

REFERENCES

[1] A. Werner, *Z. Anorg. Chem.* **1893**, *3*, 267.

[2] A. Werner, *Liebigs Ann. Chem.* **1912**, *386*, 1.

[3] S. M. Jørgensen, *Z. Anorg. Chem.* **1893**, *5*, 169.

[4] 'Perspectives in Coordination Chemistry', Eds. A. E. Williams, C. Floriani, and A. E. Merbach, Verlag Helvetica Chimica Acta, Basel, 1992.

[5] 'Comprehensive Coordination Chemistry II: From Biology to Nanotechnology', Eds. J. McCleverty and T. Meyer, Elsevier, Oxford, 2003.

[6] J. P. Hunt, H. Taube, *J. Chem. Phys.* **1951**, *19*, 602.

[7] M. Eigen, *Pure Appl. Chem.* **1963**, *6*, 97.

[8] H. R. Hunt, H. Taube, *J. Am. Chem. Soc.* **1958**, *80*, 2642.

[9] T. J. Swift, R. E. Connick, *J. Chem. Phys.* **1962,** *37*, 307; *J. Chem. Phys.* **1964**, *41*, 2553.

[10] A. E. Merbach, *Pure Appl. Chem.* **1982**, *54*, 1479.

[11] L. Helm, A. E. Merbach, D. H. Powell, in 'High-pressure Techniques in Chemistry and Physics – A Practical Approach', Vol. 2, Eds. W. B. Holzapfel and N. S. Isaacs, Oxford University Press, Oxford, 1997.

[12] S. F. Lincoln. A. E. Merbach, *Adv. Inorg. Chem.* **1995**, *42*, 1.

[13] J. E. Enderby, *Chem. Soc. Rev.* **1995**, 159.

[14] D. T. Richens, 'The Chemistry of Aqua Ions', Wiley, Chichester, 1997.

[15] L. Helm, A. E. Merbach, *Coord. Chem. Rev.* **1999**, *187*, 151.

[16] S. F. Lincoln, D. T. Richens, A. G. Sykes, 'Preparation and Properties of Aqua Ions', in 'Comprehensive Coordination Chemistry II: From Biology to Nanotechnology', Vol. 1, Section 3.1, Ed. B. Lever, Elsevier, Oxford, 2003.

[17] A. Cusanelli, U. Frey, D. T. Richens, A. E. Merbach, *J. Am. Chem. Soc.* **1996**, *118*, 5265.

[18] G. Moreau, L. Helm, J. Purans, A. E. Merbach, *J. Phys. Chem. A.* **2002**, *106*, 3034.

[19] R. D. Shannon, *Acta Crystallogr., Sect. A: Cryst. Phys., Diffr., Theor. Gen. Crystallogr.* **1976**, *32*, 751.

[20] S. T. Spees, J. R. Perumareddi, A. W. Adamson, *J. Phys. Chem.* **1968**, *72*, 1822.

[21] A. L. Companion, *J. Phys. Chem.* **1969**, *73*, 739.

[22] F. K. Meyer, K. E. Newman, A. E. Merbach, *J. Am. Chem. Soc.* **1979**, *101*, 5588.

[23] T. Kowall, F. Foglia, L. Helm, A. E. Merbach, *J. Am. Chem. Soc.* **1995**, *117*, 3790.

[24] T. Kowall, F. Foglia, L. Helm, A. E. Merbach, *J. Phys. Chem.* **1995**, 99, 13078.

[25] T. Kowall, F. Foglia, L. Helm, A. E. Merbach, *Chem.–Eur. J.* **1996**, *2*, 285.

[26] A. Bleuzen, F. Foglia, E. Furet, L. Helm, A. E. Merbach, J. Weber, *J. Am. Chem. Soc.* **1996**, *118*, 12777.
[27] F. Basolo, R. G. Pearson, 'Mechanisms of Inorganic Reactions', Wiley, 1st edn., 1957, 2nd edn, 1967.
[28] M. Eigen, K. Tamm, *Z. Elektrochem.* **1962**, 66, 93.
[29] M. Eigen, R. G. Wilkins, *Adv. Chem. Ser.* **1965**, *49*, 55.
[30] R. G. Wilkins, *Adv. Inorg. Bioinorg. Mech.* **1983**, *2*, 139.
[31] R. M. Fuoss, *J. Am. Chem. Soc.* **1958**, *80*, 5059.
[32] C. H. Langford, H. B. Gray, 'Ligand Substitution Dynamics', Benjamin, New York, 1965.
[33] C. H. Langford, W. R. Muir, *J. Am. Chem. Soc.* **1967**, *89*, 3141.
[34] J. Neely, R. E. Connick, *J. Am. Chem. Soc.* **1970**, *92*, 3476.
[35] P. J. Nichols, M. W. Grant, *Aust. J. Chem.* **1978**, *31*, 2581.
[36] J. M. Garrison, A. L. Crumbliss, *Inorg. Chem.* **1987**, *26*, 3660.
[37] R. G. Pearson, *Coord. Chem. Rev.* **1990**, *100*, 403.
[38] T. W. Swaddle, *Coord. Chem. Rev.* **1974**, *14*, 217.
[39] T. W. Swaddle, *Adv. Inorg. Bioinorg. Mech.* **1983**, *2*, 95.
[40] A. E. Merbach, *Pure Appl. Chem.* **1987**, *59*, 161.
[41] T. W. Swaddle, *Comments Inorg. Chem.* **1991**, *12*, 237.
[42] T. Kowall, P. Caravan, H. Bourgeois, L. Helm, F. P. Rotzinger, A. E. Merbach, *J. Am. Chem. Soc.* **1998**, *120*, 6569.
[43] D. Hugi Cleary, L. Helm, A. E. Merbach, *Helv. Chim. Acta* **1985**, *68*, 545.
[44] D. Hugi Cleary, L. Helm, A. E. Merbach, *J. Am. Chem. Soc.* **1987**, *109*, 4444.
[45] D. De Vito, E. Sidorenkova, F. P. Rotzinger, J. Weber, A. E. Merbach, *Inorg. Chem.* **2000**, *39*, 5547.
[46] D. De Vito, J. Weber, A. E. Merbach, *Inorg. Chem.* **2004**, *43*, 858.
[47] I. Rapaport, L. Helm, A. E. Merbach, P. Bernhard, A. Ludi, *Inorg. Chem.* **1988**, *27*, 873.
[48] G. Laurenczy, I. Rapaport, D. Zbinden, A. E. Merbach, *Magn. Reson. Chem.* **1991**, *29*, S45.
[49] P. S. Salmon, *Physica B* **1989**, *156–157*, 129.
[50] P.-A. Pittet, G. Elbaze, L. Helm, A. E. Merbach, *Inorg. Chem.* **1990**, *29*, 1936.
[51] A. Bleuzen, P.-A. Pittet, L. Helm, A. E. Merbach, *Magn. Reson. Chem.* **1997**, *35*, 765.
[52] J. P. Nordin, D. J. Sullivan, B. L. Phillips, W. H. Casey, *Inorg. Chem.* **1998**, *37*, 4760.
[53] B. Monzyk, A. L. Crumbliss, *J. Am. Chem. Soc.* **1979**, *101*, 6203.
[54] M. W. Grant, R. B. Jordan, *Inorg. Chem.* **1981**, *20*, 55.
[55] T. W. Swaddle, A. E. Merbach, *Inorg. Chem.* **1981**, *20*, 4212.
[56] A. Campisi, P. A. Tregloan, *Inorg. Chim. Acta* **1985**, *100*, 251.
[57] S. Yamada, A. Iwanagawa, S. Funahashi, M. Tanaka, *Inorg. Chem.* **1984**, *23*, 3528.
[58] F.-C. Xu, H. R. Krouse, T. W. Swaddle, *Inorg. Chem.* **1985**, *24*, 267.
[59] Y. Ducommun, D. Zbinden, A. E. Merbach, *Helv. Chim. Acta* **1982**, *65*, 1385.
[60] Y. Ducommun, K. E. Newman, A. E. Merbach, *Inorg. Chem.* **1980**, *19*, 3696.
[61] D. H. Powell, L. Helm, A. E. Merbach, *J. Chem. Phys.* **1991**, *95*, 9258.
[62] A. Pasquarello, I. Petri, P. S. Salmon, O. Parisel, R. Car, É. Tóth, D. H. Powell, L. Helm, A. E. Merbach, *Science (Washington, D.C.)* **2001**, *291*, 856.
[63] B. M. Rode, G. J. Reibnegger, S. Fujiwara, *J. Chem. Soc.*, *Faraday Trans. 2* **1980**, *76*, 1268.
[64] F. P. Rotzinger, *J. Am. Chem. Soc.* **1996**, *118*, 6760.
[65] F. P. Rotzinger, *J. Am. Chem. Soc.* **1997**, *119*, 5230.
[66] F. P. Rotzinger, *Chimia* **1997**, *51*, 97.
[67] M. Hartmann, T. Clark, R. van Eldik, *J. Am. Chem. Soc.* **1997**, *119*, 7843.
[68] E. F. Caldin, M. W. Grant, B. B. Hasinoff, *J. Chem. Soc.*, *Faraday Trans. 1* **1972**, *68*, 2247.
[69] M. W. Grant, *J. Chem. Soc.*, *Faraday Trans. 1.* **1973**, *69*, 560.
[70] E. F. Caldin, R. C. Greenwood, *J. Chem. Soc.*, *Faraday Trans. 1* **1981**, *77*, 773.
[71] R. Doss, R. van Eldik, *Inorg. Chem.* **1982**, *21*, 4108.
[72] K. Ishihara, S. Funahashi, M. Tanaka, *Inorg. Chem.* **1983**, *22*, 2564.
[73] P. J. Nichols, G. Ducommun A. E. Merbach, *Inorg. Chem.* **1983**, *22*, 3993.
[74] R. Mohr, L. A. Mietta, Y. Ducommun, R. van Eldik, *Inorg. Chem.* **1985**, *24*, 757.
[75] R. Mohr, R. van Eldik, R., *Inorg. Chem.* **1985**, *24*, 3396.
[76] Y. Ducommun, G. Laurenczy, A. E. Merbach, *Inorg. Chem.* **1988**, *27*, 1148.
[77] T. W. Kallen, J. E. Earley, *Inorg. Chem.* **1971**, *10*, 1149.
[78] N. Aebischer, G. Laurenczy, A. Ludi, A. E. Merbach, *Inorg. Chem.* **1993**, *32*, 2810.
[79] A. Desai, H. W. Dodgen, J. P. Hunt, *J. Am. Chem. Soc.* **1970**, *92*, 798.

[80] D. P. Rablen, H. W. Dodgen, J. P. Hunt, *J. Am. Chem. Soc.* **1972**, *94*, 1771.
[81] J. H. Coates, D. A. Hadi, S. F. Lincoln, H. W. Dodgen, J. P. Hunt, *Inorg. Chem.* **1981**, *20*, 707.
[82] M. Stebler-Rothlisberger, W. Hummel, P.-A. Pittet, H.-B. Bürgi, A. Ludi, A. E. Merbach, *Inorg. Chem.* **1988**, *27*, 1358.
[83] J. P. Hunt, *Coord. Chem. Rev.*, **1971**, *7*, 1.
[84] A. Neubrand, F. Thaler, M. Koerner, A. Zahl, C. D. Hubbard, R. van Eldik, *J. Chem. Soc.*, *Dalton Trans.* **2002**, 957.
[85] R. J. Cross, *Adv. Inorg. Chem.* **1989**, *34*, 219.
[86] J. Reedijk, *Proc. Natl. Acad. Sci. U.S.A.* **2003**, *100*, 3611.
[87] L. Helm, L. I. Elding, A. E. Merbach, *Helv. Chim. Acta* **1984**, *67*, 1453.
[88] L. Helm, L. I. Elding, A. E. Merbach, *Inorg. Chem.* **1985**, *24*, 1719.
[89] R. J. Deeth, L. I. Elding, *Inorg. Chem.* **1996**, *35*, 5019.
[90] L. I. Elding, L. F. Olsson, *Inorg. Chim. Acta* **1986**, *117*, 9.
[91] A. D. Hugi, L. Helm, A. E. Merbach, *Helv. Chim. Acta* **1985**, *68*, 508.
[92] A. D. Hugi, L. Helm, A. E. Merbach, *Inorg. Chem.* **1987**, *26*, 1763.
[93] P. Chaudhuri, H. Diebler, *J. Chem. Soc.*, *Dalton Trans.* **1986**, 1693.
[94] B. Perlmutter-Hayman, E. Tapuhi, *Inorg. Chem.* **1979**, *18*, 2872.
[95] P. Y. Sauvageat, Y. Ducommun, A. E. Merbach, *Helv. Chim. Acta* **1989**, *72*, 1801.
[96] B. B. Hasinoff, *Can. J. Chem.* **1979**, *57*, 77.
[97] Y. Sasaki, A. G. Sykes, *J. Chem. Soc.*, *Dalton Trans.* **1975**, 1048.
[98] D. T. Richens, Y. Ducommun, A. E. Merbach, *J. Am. Chem. Soc.* **1987**, *109*, 603.
[99] R. J. Buchacek, G. M. Harris, *Inorg. Chem.* **1976**, *15*, 926.
[100] S. C. Galbraith, C. R. Robson, D. T. Richens, *J. Chem. Soc.*, *Dalton Trans.* **2002**, 4335.
[101] L. Mønsted, O. Mønsted, *Acta Chem. Scand.* **1982**, *A36*, 555.
[102] L. Mønsted, O. Mønsted, *Coord. Chem. Rev.* **1990**, *94*, 109.
[103] T. W. Swaddle, D. R. Stranks, *J. Am. Chem. Soc.* **1972**, *94*, 8357.
[104] N. E. Brasch, D. A. Buckingham, C. R. Clark, A. Rogers, *Inorg. Chem.* **1998**, *37*, 4865.
[105] G. Gonzalez, B. Moullet, M. Martinez, A. E. Merbach, *Inorg. Chem.* **1994**, *33*, 2330.
[106] L. Dadci, H. Elias, U. Frey, A. Hornig, U. Kolele, A. E. Merbach, H. Paulus, J. S. Schneider, *Inorg. Chem.* **1995**, *34*, 306.
[107] S. Cayemittes, T. Poth, M. J. Fernandez, P. G. Lye, M. Becker, H. Elias, A. E. Merbach, *Inorg. Chem.* **1999**, *38*, 4309.
[108] K. Wüthrich, R. E. Connick, *Inorg. Chem.* **1967**, *6*, 583.
[109] Y. Kuroia, M. Harada, H. Tomiyasu, H. Fukutomi, *Inorg. Chim. Acta* **1988**, *146*, 7.
[110] M. D. Johnson, R. K. Murmann, *Inorg. Chem.* **1983**, *22*, 1068.
[111] P. Comba, A. E. Merbach, *Inorg. Chem.* **1987**, *26*, 1315.
[112] F. H. Spedding, P. F. Cullen, A. Habenschuss, *J. Chem. Phys.* **1974**, *78*, 1106.
[113] F. H. Spedding, L. E. Shiers, M. A. Brown, J. L. Derer, D. L. Swanson, A. Habenschuss, *J. Chem. Eng. Data* **1975**, *20*, 81.
[114] A. Habenschuss, F. H. Spedding, *J. Chem. Phys.* **1979**, *70*, 3758.
[115] A. Habenschuss, F. H. Spedding, *J. Chem. Phys.* **1980**, *73*, 442.
[116] T. Yamaguchi, M. Nomura, H. Wakita, H. Otaki, *J. Chem. Phys.* **1988**, *89*, 5153.
[117] K. Miyakawa, Y. Kaizu, H. Kobayashi, *J. Chem. Soc.*, *Faraday Trans.* **1988**, *84*, 1517.
[118] C. Cossy, A. E. Merbach, *Pure Appl. Chem.* **1988**, *60*, 1785.Dp
[119] C. Cossy, A. C. Barnes, J. E. Enderby, A. E. Merbach, *J. Chem. Phys.* **1989**, *90*, 3254.
[120] L. Helm, A. E. Merbach, *Eur. J. Solid State Inorg. Chem.* **1991**, *28*, 245.
[121] T. W. Swaddle, M. K. S. Mak, *Can. J. Chem.* **1983**, *61*, 473.
[122] G. Laurenczy, A. E. Merbach, *Helv. Chim. Acta* **1988**, *71*, 1971.
[123] K. Micskei, D. H. Powell, L. Helm, E. Brücher, A. E. Merbach, *Magn. Reson. Chem.* **1993**, *31*, 1011.
[124] C. Cossy, L. Helm, A. E. Merbach, *Inorg. Chem.* **1988**, *27*, 1973.
[125] C. Cossy, L. Helm, A. E. Merbach, *Inorg. Chem.* **1989**, *28*, 2699.
[126] D. H. Powell, A. E. Merbach, *Magn. Reson. Chem.* **1994**, *32*, 739.
[127] D. P. Fay, D. Litchinsky, N. Purdie, *J. Phys. Chem.* **1969**, *73*, 544.
[128] S. Galera, J. M. Lluch, A. Oliva, J. Bertran, F. Foglia, L. Helm, A. E. Merbach, *New J. Chem.* **1993**, *17*, 773.

[129] D. H. Powell, O. M. Ni Dhubhghaill, D. Pubanz, L. Helm, Y. S. Lebedev, W. Schlaepfer, A. E. Merbach, *J. Am. Chem. Soc.* **1996**, *118*, 9333.
[130] S. Zhang, M. Matthew, D. E. Woessner, R. E. Lenkinski, R. E. Sherry, *Acc. Chem. Res.* **2003**, *36*, 783.
[131] M. K. Thompson, M. Botta, G. Nicolle, L. Helm, S. Aime, A. E. Merbach, K. N. Raymond, *J. Am. Chem. Soc.* **2003**, *125*, 14274.
[132] A. E. Merbach, É. Tóth, 'The Chemistry of Contrast Agents in Medical Magnetic Resonance Imaging', Wiley, Chichester, 2001.

Received November 10, 2004